CHAPTER 4

RESULTS

This study was divided into two major parts: the in-silico and in vitro analysis. In-silico analysis identified several enriched gene ontology (GO) terms, including post-transcriptional gene silencing by RNA and miRNA-mediated suppression of translation (biological process category), as well as pathways such as Ras signalling pathway and the CML signalling pathway. In addition, KEGG pathway analysis revealed the involvement of the PI3K-AKT, ErbB, MAPK, Hedgehog, Wnt, JAK-STAT, and p53 signalling pathways, which are associated with cell cycle regulation. For the *in vitro* analysis, miRNA transfection into k562-s and k562-r cells was used to evaluate effects on cell viability, cell cycle distribution, *ABL1* and *BCR-ABL1* gene expression, and ABL1 protein expression. Notably, Osa-miR1858a/b functioned as a potential tumour suppressor, reducing cell viability by approximately 50% and inducing a G2/M phase arrest in k562-r cells. Meanwhile, the inhibition effect of hsa-miR-3131 were mostly seen on *ABL1* and *BCR-ABL1* expression in the k562-s cell. Besides. hsa-miR-3131 reduced cell viability to at least 80% in k562-s and 60% in k562-r cells. Meanwhile, hsa-miR-891a-3p reduced ABL1 gene expression and cell viability, and induced G2/M phase cell cycle arrest in K562-r cells.

4.1 In-silico Analysis

4.1.1 MiRNA-mRNA target interaction

Human and plant miRNA target interactions were determined according to their folding energy, miTG score, p-value and heteroduplex structure. Tables 4.1 and 4.2 summarise miRNA binding details on 3'UTR of the *ABL1* gene. Five plant miRNAs, the cpa-miR8154, mtr-miR2654, sof-miR59e, osa-miR1858a/b and osa-miR1858b, were predicted to have binding interactions with 3'UTR of *ABL1* gene. The best MFE score was observed in osa-miR1858a/b and osa-miR1858b at -24.4 kcal/mol, considered the lowest energy needed for miRNA to bind with the target (Table 4.1). Meanwhile, for human miRNA, DIANA tools predicted five miRNAs interacting with *ABL1*, which are the hsa-miR891a-3p, hsa-miR3131, hsa-miR6847-5p, hsa-miR1185-1-3p and hsa-miR1185-2-3p. Hsa-miR891a-3p has the highest miTG score of 0.99 with -12 kcal/mol folding energy and a p-value of 0.0037 (Table 4.2). Furthermore, hsa-mir-3131 indicated the lowest folding energy of -24.6 kcal/mol with a 0.97 miTG score. Lower folding energy is preferred for the binding between miRNA and mRNA (Saiyed et al., 2023).

Table 4.1: Plant miRNAs binding details on 3'UTR of ABL1.

miRNA	folding energy (-kcal/mol)	psRNATarget expectation score	heteroduplex	p-value	Target genes (except ABL1)
cpa-miR8154	-17.2	4	CGGCTGGTCA-CTCTGCCCTCTG || ||| |||: |||||	0.037	720
mtr-miR2654	-14.5	4	AGGGAGAAGTAGAGG-AGGAGAC AGCAC-CTT-GGCCCAGGAG |||| ||| ||| |:|	0.065	724
sof-miR159e	-14.4	4.5	GCGTGTGAAACAGGGACTTA TGTGGTTTTTTTTGAATCCAAA :|:|::|||: ||||||| TTCTCGAGGAAAG-TTAGGTTT	0.368	675
osa-miR1858a &	-24.4	4.5	GCCTC-CTTCTTCCACTTCTC |||:| ||:| ||| |:||||	0.007	720

osa-miR1858b	CGGGGTGAGGCAGGAGGAGAG

cpa: *carica papaya*, mtr: *Medicago truncatula*, sof: *Saccharum officinarum*, osa: *oryza sativa.*

Table 4.2: Human miRNAs binding details on 3'UTR of ABL1.

miRNA	folding energy (-kcal/mol)	DIANA TOOLS (miTG score)	heteroduplex	p-value	Target genes (except ABL1)
hsa-miR-891a-3p	-12	0.99	CGGGCATGCACACGGCTGGTCACT :|| :|| ||: |:||| GAGTGT-TGTTTGT-ACACGGTGA	0.037	645
hsa-miR-3131	-24.6	0.97	CCTCCCCGCTCCGTCTCTGTCCTCGA ||| ||| | |||||| TTCCGGG-AAGGTGG--TCAGGAGCT	0.037	73
hsa-miR-6847-5p	-18.8	0.95	TCTTACAAGGCC-CTTTCCTTTGG ||:||| || || |||:|| CGAGTGT-GAGGTGACAGGAGACA	0.051	992
hsa-miR-1185-1-3p	-15.7	0.92	CAAAG-CCCTGCCTCTGTGTAG ||| || ||:||||:|| TATTCTCAGAGGGGGACATATA	0.015	1850
hsa-miR-1185-2-3p	-15.5	0.92	TCAAAGCCCTGCCTCTGTGTAG || ||:||||:|| TACTCTCAGAGGGGGACATATA	0.015	1859

hsa= *homo sapiens*

4.1.2 MiRNA target genes, protein interaction network, gene ontology and pathway analysis

Each miRNA target gene was obtained by TargetRank (plant miRNA) and DIANA TOOLS, with micro-T CDS for human miRNA. The list of target genes is listed in Appendix 1. These genes were exported into STRING, and the network was later exported into Cytoscape for network analysis and protein clustering. For hsa-mir-891a-3p miRNA-targeted genes, 19 clusters were involved (Figure 4.1). Only clusters 1, 2, 3, 4, 5, 8, 9, 10 and 12 from nineteen clusters gave functional enrichment analysis data ($p<0.001$). Additionally, undirected *ABL1* first-neighbours of miR-891a-3p is displayed in Figure 4.2, with significantly enriched pathways shown in Figure 4.3.

Meanwhile, two clusters were produced for the hsa-mir-3131 targeted genes (Figure 4.4) and one cluster gave functional analysis data ($p<0.05$) with undirected *ABL1* first neighbours showed three nodes of MEF2D, NTRK2 and TCF12 and their significantly enriched pathways (Figure 4.5-4.6).

Meanwhile, from Osa-mir1858a/b targeted genes, there were eighteen clusters (Figure 4.7), with only clusters 1, 2, 3, 4, 5 and 8 giving valid enrichment data with $p<0.001$. Moreover, undirected *ABL1* first neighbours of selected nodes of osa-miR18581/b with its significantly enriched pathways are shown in Figure 4.8 and 4.9 respectively.

In Table 4.7, cluster 8 of mir-891a-3p was enriched for Reactome pathways related to miRNA biogenesis ($p=9.36x10^{-9}$) and small interfering RNA (siRNA) biogenesis ($p=1.72\ x10^{-6}$), post-transcriptional silencing by small RNAs ($p=1.13x10^{-6}$) and oncogene-induced senescence ($p=1.86x10^{-5}$), as identified by STRING enrichment analysis. The corresponding FDR-adjusted values for these pathways were all below the 0.05 significance threshold. The genes involved are AGO3, AGO1 and RAN. Respective genes are also involved in the gene ontology of the biological process of gene silencing by miRNA ($p=6.27x10^{-8}$), miRNA mediated inhibition of translation ($p=3.29x10^{-6}$) and Wnt signalling pathway ($p=2.44x10^{-5}$). Hence, these results may indicate that miR-891a-3p can inhibit gene expression and protein translation. Nevertheless, cluster 3 of osa-mir-1858a/b (Table 4.10-4.11) showed involvement in essential pathways such as pathways in cancer ($p=1.52x10^{-10}$), Ras signalling ($p=6.42x10^{-9}$), FoxO signalling ($p=8.03x10^{-9}$), PI3K-Akt signalling ($p=1.20x10^{-3}$), ErbB signalling ($p=3.01x10^{-6}$), MAPK signalling ($p=1.95x10^{-5}$), Hedgehog signalling ($p=2.67x10^{-5}$), Wnt signalling ($p=3.20x10^{-5}$), JAK-STAT signalling ($p=3.70x10^{-5}$) and p53 signalling ($p=0.0034$). Most importantly, this cluster also involves chronic myeloid

leukaemia ($p=3.18x10^{-8}$) and cell cycle pathways ($p=3.90x10^{-4}$). Thus, these findings suggest that osa-mir-1858a/b could target and bind with respective genes of the critical pathways, possibly inhibiting or disturbing such processes in the cell.

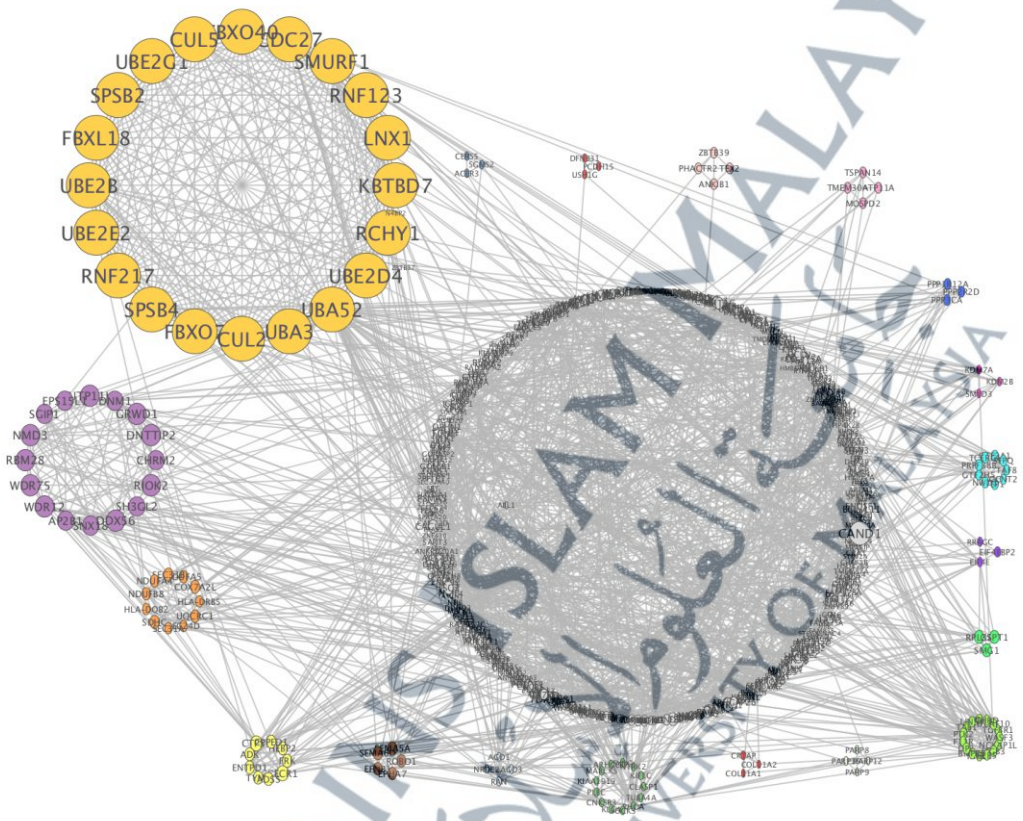

Figure 4.1: Protein–protein interaction (PPI) network clustering of hsa-miR-891a-3p target genes showing 19 clusters. The network was generated and visualised in Cytoscape. Clusters were identified using the MCODE plugin, with node colours representing distinct functional modules and node size indicating connection degree.

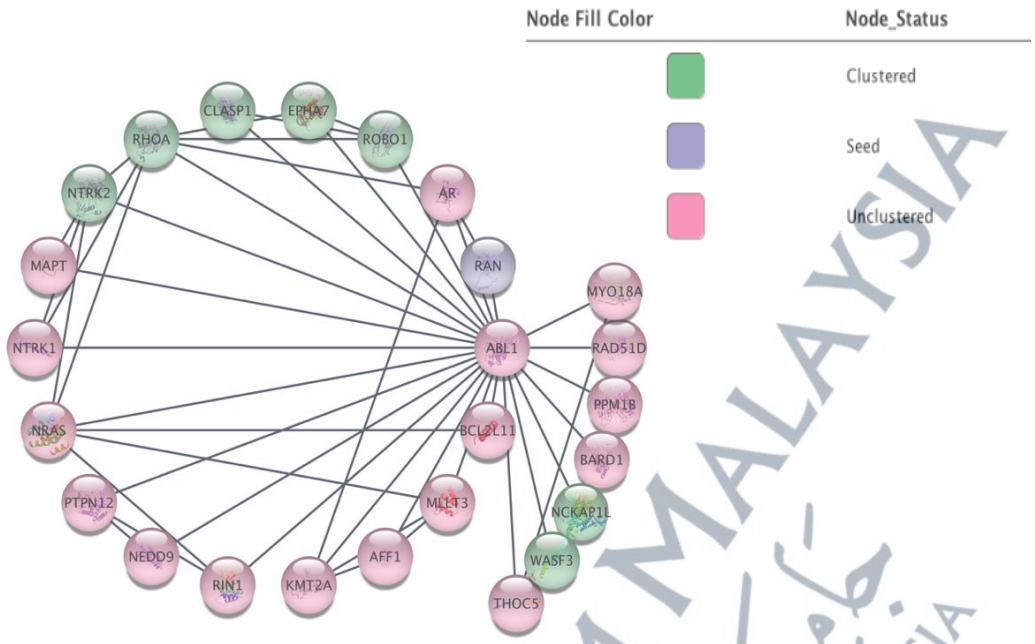

Figure 4.2: Undirected *ABL1* first-neighbours network of hsa-mir-891a-3p. The network was generated using Cytoscape, showing protein-protein interactions between ABL1 and its first neighbours.

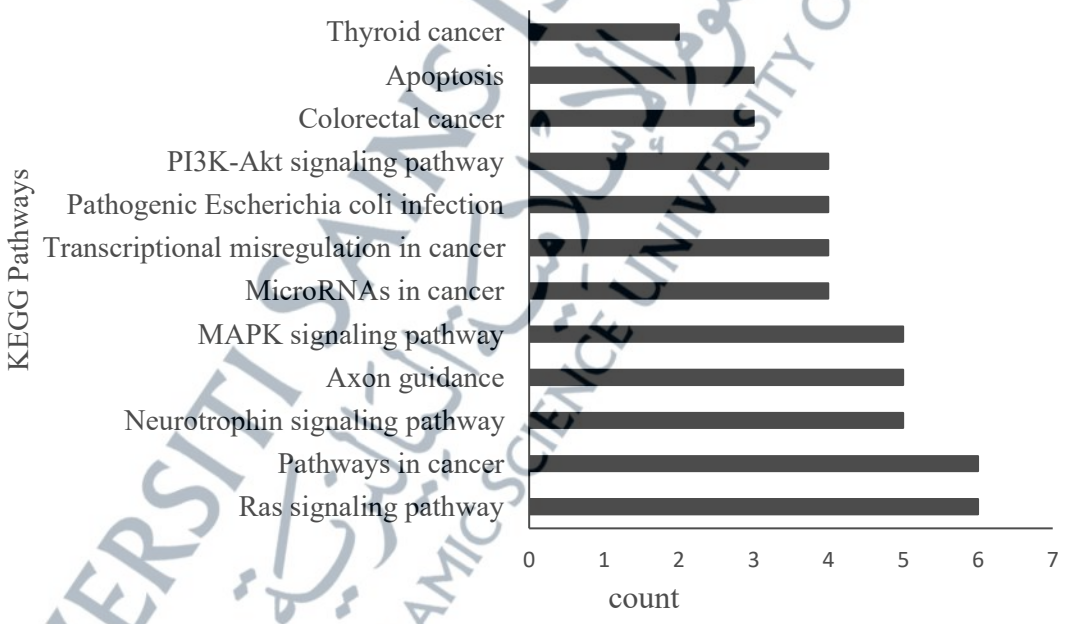

Figure 4.3: Significantly enriched pathways based on the p-value of the undirected first neighbours of ABL1 in the hsa-mir-891a-3p network.

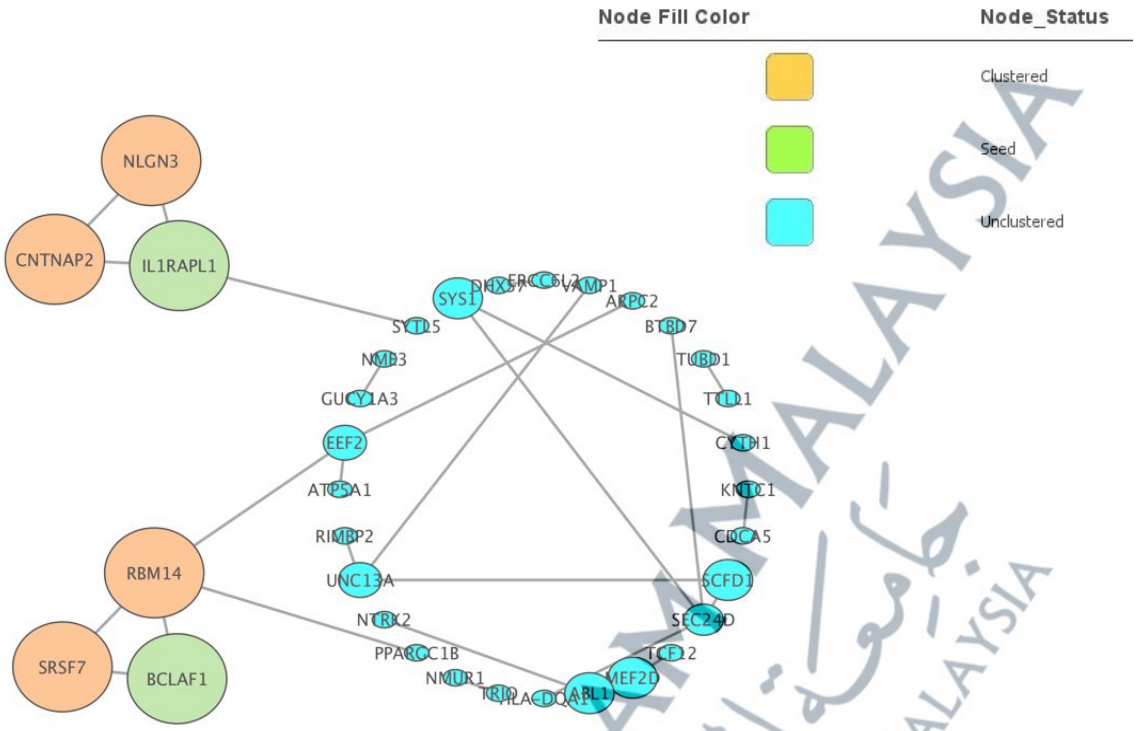

Figure 4.4: Protein–protein interaction (PPI) network clustering of hsa-miR-3131 target genes showing two clusters. The network was generated and visualised in Cytoscape. Clusters were identified using the MCODE plugin, with node colours representing distinct functional modules and node size indicating connection degree.

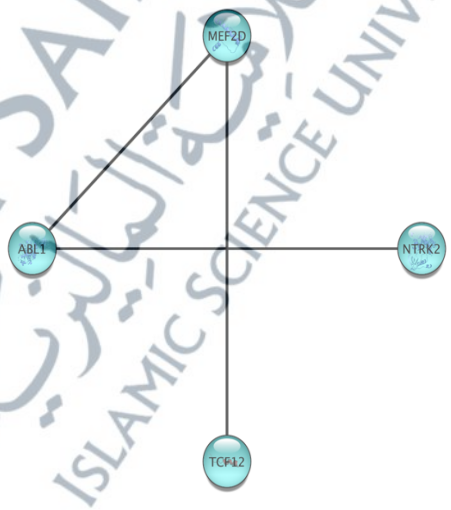

Figure 4.5: Undirected ABL1 first-neighbours network of hsa-mir-3131. The network was generated using Cytoscape, showing protein-protein interactions between ABL1 and its first neighbours.

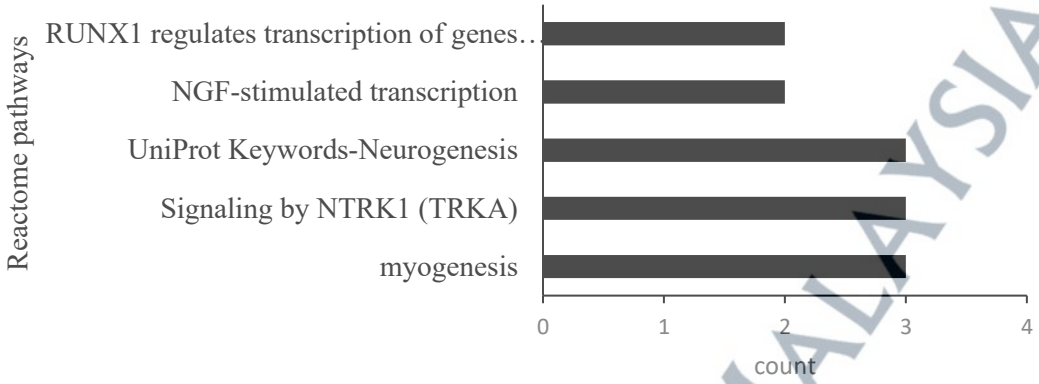

Figure 4.6: Significantly enriched pathways based on the p-value of the undirected first neighbours of ABL1 in the hsa-mir3131 network.

Figure 4.7: Protein–protein interaction (PPI) network clustering of Osa-miR-1858a/b target genes showing 18 clusters. The network was generated and visualised in Cytoscape. Clusters were identified using the MCODE plugin, with node colours representing distinct functional modules and node size indicating connection degree.

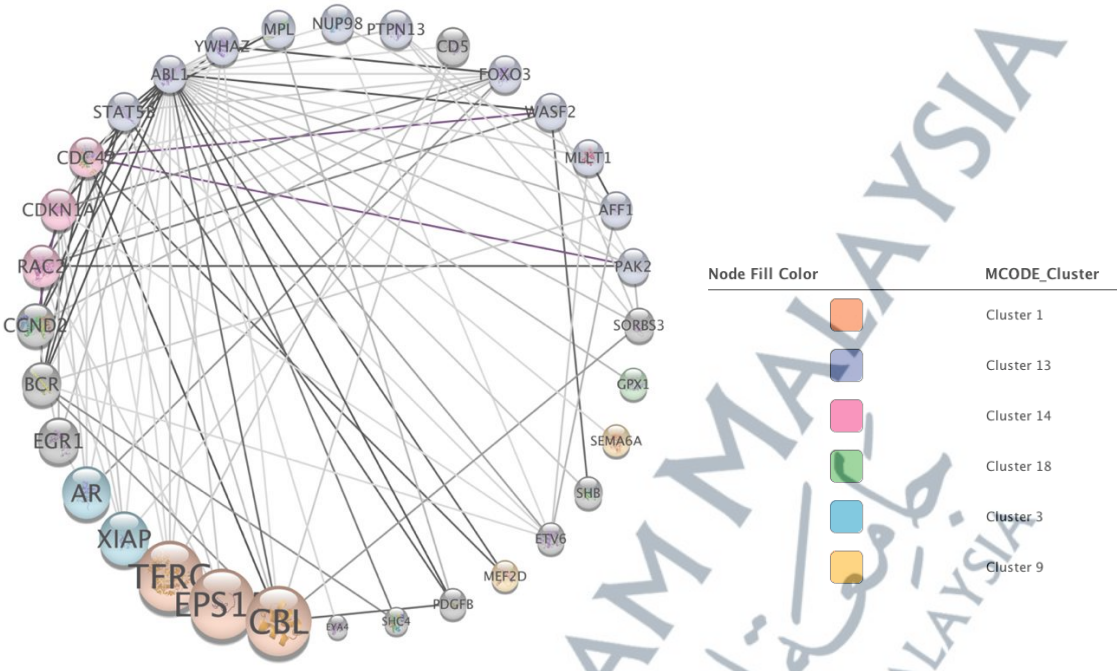

Figure 4.8:Undirected ABL1 first-neighbours network of Osa-miR-1858a/b. The network was generated using Cytoscape, showing protein-protein interactions between ABL1 and its first neighbours.

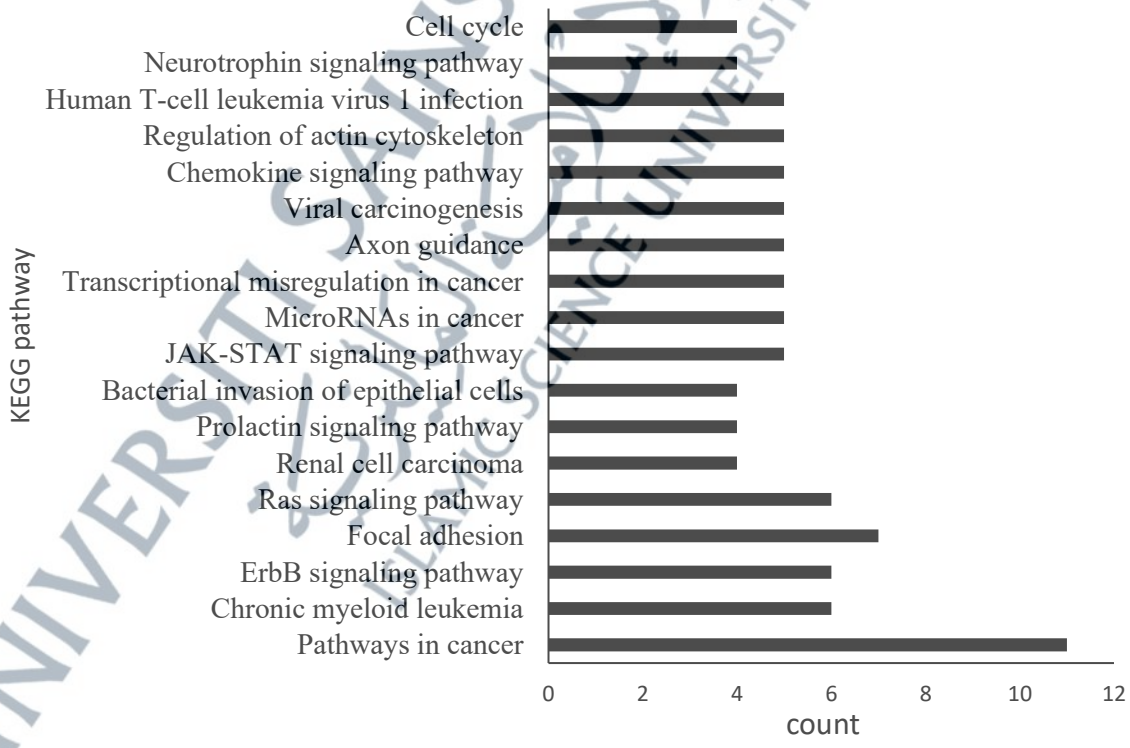

Figure 4.9: Significantly enriched pathways based on the P-value of the undirected first neighbours of ABL1 in the Osa-mir-1858a/b network.

Table 4.3: Functional enrichment table of miRNA's cluster.

miRNA	Cluster		Description	Genes	p-value
Hsa-miR-891a-3p	Cluster 1	Reactome pathways	Antigen processing: Ubiquitination & Proteasome degradation	*UBE2D4, LNX1, UBE2B, FBXO7, SPSB4, RCHY1, RNF123, FBXO40, UBA3, SMURF1, KBTBD7, FBXL18, CUL5, UBE2E2, UBE2G1, UBA52, SPSB2, RNF21, CDC27, CUL2.*	1.31E-36
			Synthesis of active ubiquitin: roles of E1 and E2 enzymes	*UBE2B, UBE2G1, UBA52.*	4.87E-06
		Biological Process	Post-translational protein modification	*FBXO7, SPSB4, FBXO40, UBA3, KBTBD7, FBXL18, CUL5, SPSB2, CUL2*	3.80E-11
			Positive regulation of ubiquitin-dependent protein catabolic process	*RCHY1, SMURF, RNF217, CDC27*	5.82E-06
		Molecular function	Ubiquitin protein ligase binding	*UBE2D4, UBE2B, FBXO7, CUL5, UBE2G1, UBA52, CUL2*	1.29E-08
		Compartment	Ubiquitin ligase complex	*UBE2B, FBXO7, RCHY1, KBTBD7, FBXL18, CUL5, CDC27, CUL2*	9.22E-11
	Cluster 2	KEGG pathways	Ribosome biogenesis in eukaryotes	*RBM28, RIOK2, WDR75, NMD3*	4.76E-07
			Endocytosis	*DNM1, SH3GL2, EPS15L1, AP2B1*	3.87E-05
		GO Biological Process	Ribosome biogenesis	*DDX56, WDR12, RIOK2, WDR75, UTP11L, NMD3*	8.32E-08
			rRNA processing	*DDX56, WDR12, RIOK2, WDR75, UTP11L*	6.31E-07
			Endocytosis	*SNX18, SGIP1, DNM1, SH3GL2,EPS15L1,AP2B1*	8.12E-07

The p-values shown are raw values generated by STRING enrichment analysis. Multiple testing correction was performed using the Benjamini–Hochberg false discovery rate (FDR) method. All pathways/gene ontology terms listed met the significance threshold of FDR < 0.05. Corresponding FDR values are available upon request.

Table 4.4: Functional enrichment table of miRNA's cluster (continued).

miRNA	Cluster		Description	Genes	p-value
Hsa-miR-891a-3p	Cluster 2	GO Biological Process	Membrane organization	*SNX18,SGIP1,DNM1,SH3GL2,EPS15L1,CHRM2,AP2B1*	1.57E-06
			Cellular component organization or biogenesis	*GRWD1,DDX56,WDR12,RIOK2,WDR75,SNX18,SGIP1,DNM1,UTP11L,SH3GL2,EPS15L1,CHRM2,NMD3,AP2B1*	1.75E-06
			Cellular component biogenesis	*GRWD1,DDX56,WDR12,RIOK2,WDR75,SGIP1,UTP11L,SH3GL2,NMD3,AP2B1*	6.09E-06
			Synaptic vesicle endocytosis	*DNM1,SH3GL2,AP2B1*	9.10E-06
			Regulation of endocytosis	*SGIP1,DNM1,SH3GL2,AP2B1*	2.08E-05
			Postsynaptic neurotransmitter receptor internalization	*DNM1,AP2B1*	2.81E-05
			RNA processing	*RBM28,DDX56,WDR12,RIOK2,WDR75,UTP11L*	3.87E-05
			Regulation of vesicle-mediated transport	*SGIP1,DNM1,SH3GL2,CHRM2,AP2B1*	6.05E-05
		GO Cellular Component	Nucleolus	*RBM28,GRWD1,DDX56,WDR12,WDR75,UTP11L,DNTTIP2,NMD3*	2.34E-07
			Membrane coat	*SGIP1,DNM1,EPS15L1,AP2B1*	9.44E-07
			Cytoplasmic vesicle membrane	*SNX18,SGIP1,SH3GL2,CHRM2,AP2B1*	2.90E-04
			Membrane-bounded organelle	*RBM28,GRWD1,DDX56,WDR12,RIOK2,WDR75,SNX18,SGIP1,DNM1,UTP11L,SH3GL2,EPS15L1,CHRM2,DNTTIP2,NMD3,AP2B1*	7.00E-04
			Presynapse	*DNM1,SH3GL2,CHRM2,AP2B1*	7.50E-04
			Preribosome	*WDR12,RIOK2,UTP11L*	3.67E-05

Table 4.5: Functional enrichment table of miRNA's cluster (continued).

miRNA	Cluster		Description	Genes	p-value
Hsa-miR-891a-3p	Cluster 3	KEGG pathways	Oxidative phosphorylation	*UQCRC1,NDUFB8,NDUFA4,SDHC,COX7A2L,NDUFA5*	4.52E-11
			Protein processing in the endoplasmic reticulum	*SEC24D,SEC31B,SEC31A*	9.74E-05
			Thermogenesis	*UQCRC1,NDUFB8,NDUFA4,SDHC,COX7A2L,NDUFA5*	1.23E-09
			Metabolic pathways	*UQCRC1,NDUFB8,NDUFA4,SDHC,COX7A2L,NDUFA5*	5.52E-05
		Go biological process	Mitochondrial ATP synthesis coupled electron transport	*UQCRC1,NDUFB8,NDUFA4,SDHC,COX7A2L,NDUFA5*	4.42E-12
			Aerobic respiration	*UQCRC1,NDUFA4,SDHC,COX7A2L*	9.69E-08
			Antigen processing and presentation of exogenous peptide antigen via MHC class ii	*SEC24D,HLA-DRB5,SEC31A,HLA-DQB2*	2.06E-07
			Mitochondrial electron transport, NADH to ubiquinone	*NDUFB8,NDUFA4,NDUFA5*	2.87E-06
			Mitochondrial electron transport, cytochrome c to oxygen	*NDUFA4,COX7A2L*	6.59E-05
		GO Molecular Function	Oxidoreductase activity	*UQCRC1,NDUFB8,NDUFA4,SDHC,COX7A2L,NDUFA5*	1.05E-06
			NADH dehydrogenase (ubiquinone) activity	*NDUFB8,NDUFA4,NDUFA5*	2.40E-06
			Electron transfer activity	*UQCRC1,SDHC,COX7A2L*	2.47E-05
		GO cellular component	Membrane protein complex	*UQCRC1,SEC24D,NDUFB8,NDUFA4,SDHC,SEC31B,HLA-DRB5,SEC31A,HLA-DQB2,NDUFA5*	4.95E-12
			ER to Golgi transport vesicle membrane	*SEC24D,SEC31B,HLA-DRB5,SEC31A,HLA-DQB2*	1.34E-10

Table 4.6: Functional enrichment table of miRNA's cluster (continued).

miRNA	Cluster		Description	Genes	p-value
Hsa-miR-891a-3p	Cluster 3	GO cellular component	Respiratory chain complex	*UQCRC1,NDUFB8,NDUFA4,SDHC,NDUFA5*	6.20E-10
			Oxidoreductase complex	*UQCRC1,NDUFB8,NDUFA4,SDHC,NDUFA5*	2.52E-09
			Organelle membrane	*UQCRC1,SEC24D,NDUFB8,NDUFA4,SDHC,SEC31B,HLA-DRB5,COX7A2L,SEC31A,HLA-DQB2,NDUFA5*	7.08E-09
			Inner mitochondrial membrane protein complex	*UQCRC1,NDUFB8,NDUFA4,SDHC,NDUFA5*	6.71E-09
	Cluster 4	KEGG Pathways	Purine metabolism	*ADK,ADSS,ENTPD1,CECR1*	2.35E-07
			Pyrimidine metabolism	*TYMS,ENTPD1,CTPS1*	2.16E-06
			Metabolic pathways	*ADK,TYMS,ADSS,ENTPD1,CTPS1,CECR1*	1.14E-05
		GO Biological Process	Nucleobase-containing small molecule metabolic process	*ADK,TYMS,ADSS,ENTPD1,CTPS1,CECR1*	2.50E-08
			Nucleoside monophosphate biosynthetic process	*ADK,TYMS,ADSS*	1.01E-06
			AMP biosynthetic process	*ADK,ADSS*	3.94E-06
		Compartments	Lysosome	*CPPED1,CECR1,HEBP2,FRK*	6.80E-05
			Vacuole	*CPPED1,CECR1,HEBP2,FRK*	1.10E-04
			Secretory granule	*CPPED1,CECR1,HEBP2,FRK*	1.80E-04
	Cluster 5	KEGG Pathways	Axon guidance	*EFNB1,SEMA6D,EPHA7,SEMA5A,ROBO1*	6.58E-11
		GO Biological Process	Axon guidance	*EFNB1,SEMA6D,EPHA7,SEMA5A,ROBO1*	5.79E-10
			Regulation of axonogenesis	*SEMA6D,EPHA7,SEMA5A,ROBO1*	4.36E-08
			Negative chemotaxis	*SEMA6D,EPHA7,ROBO1*	1.29E-07
		GO Molecular Function	Axon guidance receptor activity	*EPHA7,ROBO1*	2.87E-06

Table 4.7: Functional enrichment table of miRNA's cluster (continued).

miRNA	Cluster		Description	Genes	p-value
Hsa-miR-891a-3p	Cluster 8	Reactome pathways	MicroRNA (miRNA) biogenesis	*AGO3,AGO1,RAN*	9.36E-09
			Small interfering RNA (siRNA) biogenesis	*AGO3,AGO1*	1.72E-06
			Post-transcriptional silencing by small RNAs	*AGO3,AGO1*	1.13E-06
			Oncogene Induced Senescence	*AGO3,AGO1*	1.86E-05
			Transcriptional regulation by small RNAs	*AGO1,RAN*	9.36E-05
			TP53 Regulates Metabolic Genes	*AGO3,AGO1*	1.20E-04
			MAPK6/MAPK4 signaling	*AGO3,AGO1*	1.20E-04
			Oxidative Stress-induced senescence	*AGO3,AGO1*	1.40E-04
	Cluster 8	GO Biological Process	Post-transcriptional gene silencing by RNA	*NRDE2,AGO3,AGO1,RAN*	8.54E-11
			Gene silencing by miRNA	*AGO3,AGO1,RAN*	6.27E-08
			miRNA loading onto RISC involved in gene silencing by miRNA	*AGO3,AGO1*	1.13E-06
			RNA secondary structure unwinding	*AGO3,AGO1*	1.41E-06
			pre-miRNA processing	*AGO3,AGO1*	3.76E-06
			MiRNA-mediated inhibition of translation	*AGO3,AGO1*	3.29E-06
			miRNA metabolic process	*AGO1,RAN*	8.64E-06
			Wnt signalling pathway, calcium modulating pathway	*AGO3,AGO1*	2.44E-05
			Ribonucleoprotein complex biogenesis	*AGO3,AGO1,RAN*	4.03E-05
			ncRNA metabolic process	*AGO3,AGO1,RAN*	5.41E-05
			Positive regulation of nucleocytoplasmic transport	*NRDE2,RAN*	7.32E-05

Table 4.8: Functional enrichment table of miRNA's cluster (continued).

miRNA	Cluster		Description	Genes	p-value
	Cluster 9	Reactome Pathways	Maturation of nucleoprotein	*PARP16,PARP8,PARP9*	9.16E-10
		GO Cellular Component	Endoplasmic reticulum tubular network	*PARP16,PARP8*	1.27E-05
		GO Molecular Function	Protein serine/threonine kinase activator activity	*PARP16,PARP8*	2.96E-05
	Cluster 10	KEGG Pathways	TGF-beta signalling pathway	*CHRD,INHBB,BMPR2,TGFBR1,E2F5*	4.93E-09
			Cellular senescence	*LIN9,LIN54,TGFBR1,E2F5*	3.46E-06
		GO Biological Process	Transmembrane receptor protein serine/threonine kinase signalling pathway	*CHRD,TAB1,INHBB,F11R,BMPR2,TGFBR1*	3.05E-09
			Enzyme-linked receptor protein signalling pathway	*CHRD,TAB1,NCKAP1L,INHBB,F11R,BMPR2,TGFBR1,ITGB3*	8.66E-09
	Cluster 12	GO Biological Process	RNA metabolic process	*CCNT2,TCERG1,SFPQ,PRPF38B,TAF8,GTF2A1,GTF2H5*	7.20E-07
			Gene expression	*CCNT2,TCERG1,SFPQ,PRPF38B,TAF8,GTF2A1,GTF2H5*	4.25E-06
			snRNA transcription by RNA polymerase II	*CCNT2,TAF8,GTF2A1*	4.29E-06
		GO Cellular Component	Transcription factor complex	*TAF8,GTF2A1,GTF2H5*	6.09E-07
			RNA polymerase II transcription regulator complex	*SFPQ,TAF8,GTF2A1,GTF2H5*	6.23E-07
			Transferase complex, transferring phosphorus-containing groups	*CCNT2,TAF8,GTF2A1,GTF2H5*	2.78E-06

Table 4.9: Functional enrichment table of miRNA's cluster (continued).

miRNA	Cluster		Description	Genes	p-value
hsa-miR-3131	Cluster 2	KEGG pathways	Cell adhesion molecules (CAMs)	*NLGN3,CNTNAP2*	1.50E-04
		Reactome pathways	Protein-protein interactions at synapses	*NLGN3,IL1RAPL1*	5.84E-05
			Neuronal System	*NLGN3,IL1RAPL1*	0.001
		GO process	presynaptic membrane assembly	*NLGN3,IL1RAPL1*	8.62E-07
			cell adhesion	*NLGN3,CNTNAP2,IL1RAPL1*	8.05E-05
		GO Component	cell surface	*NLGN3,CNTNAP2,IL1RAPL1*	4.42E-05
			plasma membrane region	*NLGN3,CNTNAP2,IL1RAPL1*	1.60E-04
			postsynaptic membrane	*NLGN3,IL1RAPL1*	4.40E-04
			plasma membrane part	*NLGN3,CNTNAP2,IL1RAPL1*	0.0025
			dendrite	*CNTNAP2,IL1RAPL1*	0.0022
			axon	*CNTNAP2,IL1RAPL1*	0.0022
			synapse part	*NLGN3,IL1RAPL1*	0.0038
			cell junction	*NLGN3,CNTNAP2*	0.0077
Osa-miR1858a/b and osa-miR1858b (18 clusters)	Cluster 1	KEGG pathways	Synaptic vesicle cycle	*SLC17A7,CPLX1,VAMP2,CPLX2,UNC13B*	4.27E-10
		WikiPathways	Synaptic vesicle pathway	*SLC17A7,SNAP25,SYP,CPLX1,VAMP2,CPLX2,UNC13B,SYN2*	6.80E-19
		GO Biological Process	Regulation of neurotransmitter levels	*SLC17A7,SNAP25,SYP,CPLX1,VAMP2,CPLX2,SYT11,UNC13B,VAMP1,SYN2*	7.21E-19
			Synaptic vesicle cycle	*SLC17A7,SNAP25,SYP,CPLX1,VAMP2,CPLX2,UNC13B,VAMP1,SYN2*	9.59E-19
			Regulation of synaptic vesicle cycle	*SLC17A7,SYP,BSN,CPLX1,CPLX2,SYT11,UNC13B,VAMP1*	2.93E-16

Table 4.10: Functional enrichment table of miRNA's cluster (continued).

miRNA	Cluster		Description	Genes	p-value
Osa-miR1858a/b and osa-miR1858b (18 clusters)	Cluster 1	GO Cellular Component	Presynapse	*SLC17A7,SNAP25,SYP,BSN,CPLX1,VAMP2,CPLX2,SYT11,UNC13B,VAMP1,SYN2*	5.98E-18
			Synaptic vesicle	*SLC17A7,SNAP25,SYP,BSN,VAMP2,SYT11,UNC13B,VAMP1,SYN2*	9.32E-17
			Synaptic vesicle membrane	*SLC17A7,SYP,BSN,VAMP2,UNC13B,VAMP1,SYN2*	5.37E-14
	Cluster 2	KEGG Pathways	Ribosome biogenesis in eukaryotes	*UTP15,GNL3L,WDR36*	2.27E-06
		Reactome Pathways	rRNA modification in the nucleus and cytosol	*KRR1,UTP15,WDR36*	1.10E-06
			Major pathway of rRNA processing in the nucleolus and cytosol	*KRR1,UTP15,WDR36*	2.74E-05
			Metabolism of RNA	*TRMT6,KRR1,UTP15,WDR36*	4.21E-05
		GO Biological Process	Ribosome biogenesis	*KRR1,UTP15,GNL3L,TSR2,WDR36*	1.59E-08
			ncRNA processing	*TRMT6,KRR1,UTP15,TSR2,WDR36*	5.91E-08
			rRNA processing	*KRR1,UTP15,TSR2,WDR36*	4.92E-07
	Cluster 3	KEGG Pathways	Pathways in cancer	*GNB4,CCND2,AKT3,ARAF,STAT5B,PRKACA,SMAD3,GNG2,PRKACB,CDKN1A*	1.52E-10
			Ras signalling pathway	*GNB4,AKT3,PRKACA,GNG2,PRKACB,KSR2,BDNF*	6.42E-09
			FoxO signalling pathway	*CCND2,AKT3,ARAF,SMAD3,CDKN1A,FOXO3*	8.03E-09
			Chronic myeloid leukaemia	*AKT3,ARAF,STAT5B,SMAD3,CDKN1A*	3.18E-08
			PI3K-Akt signalling pathway	*GNB4,CCND2,AKT3,GNG2,CDKN1A,FOXO3,BDNF*	1.20E-07
			Cellular senescence	*CCND2,AKT3,SMAD3,CDKN1A,FOXO3*	8.72E-07
			ErbB signalling pathway	*AKT3,ARAF,STAT5B,CDKN1A*	3.01E-06
			MAPK signalling pathway	*AKT3,ARAF,PRKACA,PRKACB,BDNF*	1.95E-05
			Hedgehog signalling pathway	*CCND2,PRKACA,PRKACB*	2.67E-05

Table 4.11: Functional enrichment table of miRNA's cluster (continued).

miRNA	Cluster		Description	Genes	p-value
Osa-miR1858a/b and osa-miR1858b (18 clusters)	Cluster 3	KEGG Pathways	Wnt signalling pathway	*CCND2,PRKACA,SMAD3,PRKACB*	3.20E-05
			JAK-STAT signalling pathway	*CCND2,AKT3,STAT5B,CDKN1A*	3.70E-05
			Cell cycle	*CCND2,SMAD3,CDKN1A*	3.90E-04
			p53 signalling pathway	*CCND2,CDKN1A*	0.0034
		GO Molecular Function	Protein kinase binding	*CCND2,PRKACA,SMAD3,DCX,FOXM1,TBR1,CDKN1A,FOXO3*	5.04E-07
			Protein kinase activity	*AKT3,ARAF,PRKACA,PRKACB,CDKN1A,KSR2*	4.07E-05
			cAMP-dependent protein kinase activity	*PRKACA,PRKACB*	4.72E-05
			Protein serine/threonine kinase activity	*AKT3,ARAF,PRKACA,PRKACB,KSR2*	1.40E-04
	Cluster 4	GO Cellular Component	Synapse	*PSD2,SLC1A2,GABRG1,FAIM2,KCNJ10*	1.59E-06
			Plasma membrane region	*PSD2,SLC1A2,GABRG1,FAIM2,KCNJ10*	9.50E-07
		GO Biological Process	L-glutamate import across the plasma membrane	*SLC1A2,KCNJ10*	1.88E-06
			Neurotransmitter reuptake	*SLC1A2,KCNJ10*	1.09E-05
	Cluster 5	GO Biological Process	Regulation of cell shape	*RAC2,PLXNA2,PLXNA3,DIAPH1*	3.74E-06
			Cellular component morphogenesis	*RAC2,ANK2,PLXNA2,PLXNA3,SPTB,WASF2*	2.38E-06
			Golgi vesicle transport	*ARF3,ARCN1,ANK1,ANK2,SPTB*	3.77E-06
			Endoplasmic reticulum to golgi vesicle-mediated transport	*ARCN1,ANK1,ANK2,SPTB*	9.57E-06
			Vesicle-mediated transport	*RAC2,ARF3,ARCN1,ANK1,ANK2,DIAPH1,SPTB,WASF2*	9.59E-06
			Plasma membrane-bounded cell projection morphogenesis	*RAC2,PLXNA2,PLXNA3,SPTB,WASF2*	1.83E-05
	Cluster 8	KEGG Pathways	ErbB signaling pathway	*MAPK1,PAK2,MAP2K4*	1.40E-04
			MAPK signalling pathway	*MAPK1,PAK2,MAPKAPK2,MAP2K4*	3.40E-04

Table 4.12: Functional enrichment table of miRNA's cluster (continued).

miRNA	Cluster		Description	Genes	p-value
Osa-miR1858a/b and osa-miR1858b (18 clusters)	Cluster 8	KEGG Pathways	VEGF signalling pathway	*MAPK1,MAPKAPK2*	0.0022
		GO Molecular Function	MAP kinase kinase activity	*MAPK1,MAP2K4*	2.50E-04
			Mitogen-activated protein kinase kinase kinase binding	*MAPK1,MAP2K4*	2.50E-04

The p-values shown are raw values generated by STRING enrichment analysis. Multiple testing correction was performed using the Benjamini–Hochberg false discovery rate (FDR) method. All pathways/gene ontology terms listed met the significance threshold of FDR < 0.05. Corresponding FDR values are available upon request.

4.2 Transfection Efficiency and Target Site Validation

4.2.1 MicroRNA TaqMan Assay

Transfection efficiency was assessed by quantifying intracellular miRNA levels. Custom-designed miRNA primers and TaqMan probe for hsa-miR-3131, hsa-miR-891a-3p and osa-miR1858a/b were used to measure the amount of miRNA successfully transfected into the cells. Total miRNA was extracted, reverse-transcribed to cDNA, and amplified according to the manufacturer's protocols. Cq values were calculated, compared with the untreated groups, and normalised to RNU48 as the housekeeping miRNA.

As shown in Figure 4.10 and Figure 4.11, all miRNAs displayed significantly higher expression in both cell lines compared to the untreated group ($p<0.05$). In k562-s, the mean ± SD expression were: hsa-miR-3131 (3275.6 ± 364.2), hsa-miR-891a-3p (1190.8 ± 641.2) and osa-1858a/b (924.7 ± 393.7). In K562-r, the corresponding value were: hsa-miR-3131 (96,539.4 ± 15,212.6), hsa-miR-891a-3p (49,991.5 ± 28,901.7) and osa-1858a/b (35,8226.8 ± 51,583.4). The untreated group's expression is not visible in the graph due to extremely low levels relative to the treated groups. These high levels of miRNA confirmed successful transfection and intracellular transport of the miRNAs. Among the treated samples, K562-r cells showed higher miRNA expression than K562-s cells, indicating greater transfection efficiency in the resistant cell line.

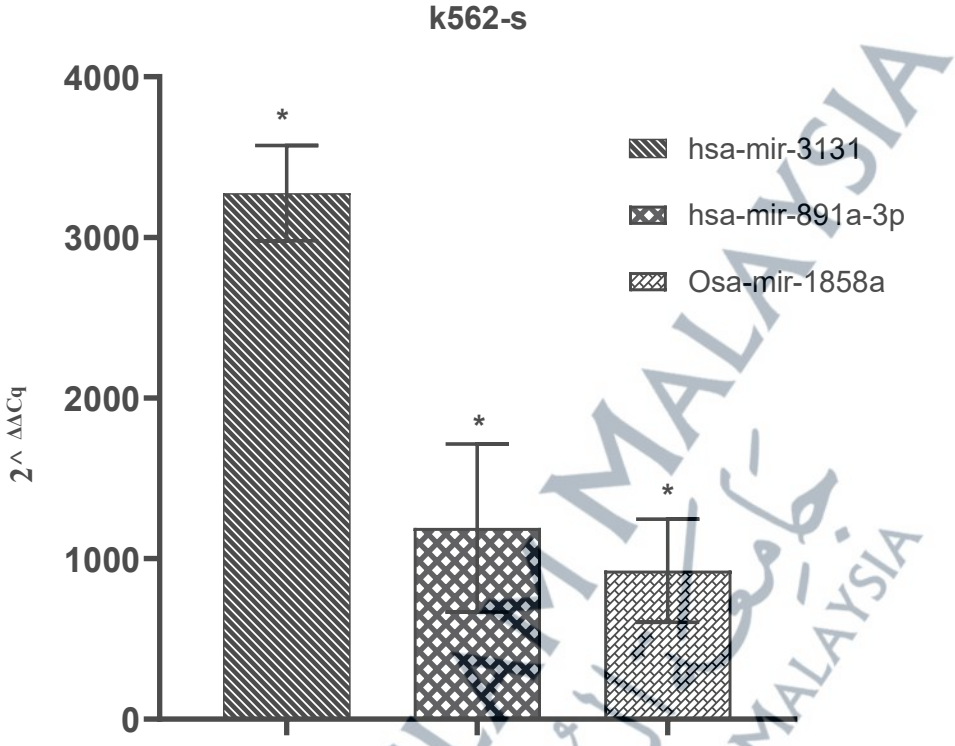

Figure 4.10: miRNA levels after transfection in the K562-s cells. Data are expressed as $2^{-\Delta\Delta Cq}$ value ± SD from two biological replicates. *p<0.05 compared to untreated.

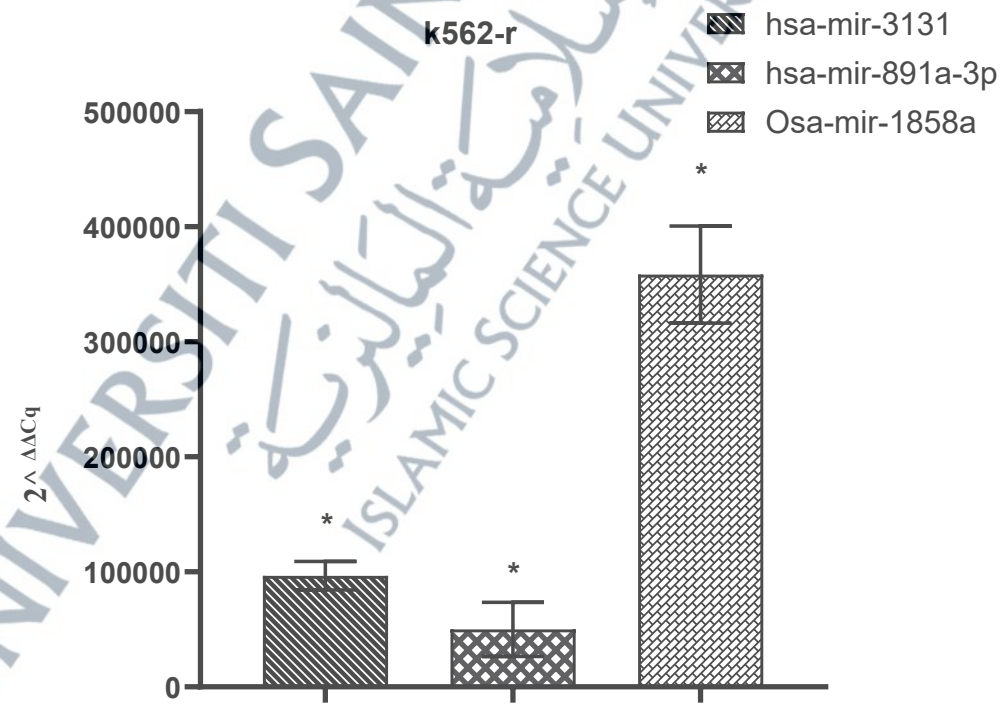

Figure 4.11: MiRNA levels after transfection in the K562-r cell. Data are expressed as $2^{-\Delta\Delta Cq}$ value ± SD from two biological replicates. *p<0.05 compared to untreated.

4.2.2 Biotin-based pulldown assay

An assay of Biotin pull-down assay was used to validate the miRNA-mRNA target binding at the 3'UTR. This assay is an alternative to the commonly used method of Luciferase assay. This is due to the less amount of time and less complexity compared to luciferase assay, which is known to be laborious and time-consuming (Li et al., 2023). Biotin-labelled miRNA pull-down is a valuable method for identifying miRNA target genes under conditions that closely mimic endogenous cellular processes. Furthermore, it has been observed by researchers that there has been a gradual rise in the utilisation of biotin-labelled miRNA pull-down due to its notable specificity in identifying unique miRNA target genes (Awan et al., 2018; Ørom & Lund, 2007).

A qPCR assay successfully detected target mRNA bound to miRNAs from the pull-down mixture. Primers were specifically designed to target the 3'UTR regions of *ABL1* and their sequences are listed in Table 4.13. The qPCR gene expression results were compared against two control groups: (i) the control lysate group (before pull-down) and (ii) the non-transfected group. Only two miRNAs, hsa-miR-3131 and hsa-miR-891-3p were validated through this method. Osa-miR1858a/b was not validated due to the unavailability of biotin-tag plant-derived miRNAs.

RNA was extracted from samples using modified RNA clean-up protocols. This adjustment was necessary because the mRNA was bound to miRNA attached to biotin, which in turn was pulled using the streptavidin magnetic beads. Since the RNA was attached to the beads, the extraction process was optimised to ensure complete detachment before continuing with the subsequent RNA purification steps.

Table 4.14 present the extracted RNA concentration and quality. The RNA concentration after pull-down was lower than before pull-down because only RNA molecules bound to the biotin-labelled miRNA (and thus retained by the magnetic

beads) were recovered. This selective capture process inherently reduces the total RNA yield compared to the pre-pull-down lysate, which contains all cellular RNA.

Figure 4.12 and 4.13 shows the same experimental groups but with different control references. Figure 4.12 compares pull-down samples to the control lysate (RNA before pull-down), allowing assessment of target enrichment relative to the input material. Figure 4.13 compares the same samples to the untreated (non-transfected) group, representing baseline expression without miRNA transfection. Using both controls enables evaluation of enrichment against both technical and biological backgrounds. In k562-s cells, no significant difference in target gene expressions was observed between treatment groups and control lysate (before pull-down) for either mir-3131 and mir-891a-3p (Figure 4.12). Although mir-891a-3p showed a higher trend compared to control lysate, this difference was not significant. However, when compared to the non-transfected control group, miR-891-3p exhibited significantly higher 3'UTR ABL1 expression ($p<0.05$), whereas miR-3131 remained non- significant (Figure 4.13).

In k562-r cells (Figure 4.14 and 4.15), both hsa-miR-3131 and hsa-miR-891-3p displayed significantly higher 3'UTR ABL1 expression group compared to both control lysate and untreated group ($p<0.05$,). These findings suggest that the target interaction between miRNAs and the ABL1 3'UTR was successfully validated in K562-r cells for both miRNAs, whereas in k562-s cells, validation was only observed for miR-891a-3p when compared to the untreated control.

Table 4.13: List of primers for biotin pull-down assay validation.

Gene	Forward Primer sequence (5' to 3')	Reverse Primer sequence (5' to 3')
3'UTR ABL1 mir-3131	TCCCGCACCTTCCTCCTC	CTCAGTCTGGGGCACTAGGT
3'UTR ABL1 mir-891a-3p	CCTGCCTCTGTGTAGCCG	CCTTTCCTCCCACCTGTGC

Table 4.14: RNA concentration and quality.

Sample Name	RNA concentration (ng/µl)	A260/280	A260/230
Before pull-down			
S2 3131 CL	23.6	1.96	0.79
S3 3131 CL	60.4	1.98	1.91
S2 891 CL	78.0	2.01	1.69
S3 891 CL	16.0	1.90	0.07
S4 891 CL	10.0	1.78	0.58
R1 3131 CL	48.8	2.00	1.20
R2 3131 CL	33.6	2.04	0.92
R3 3131 CL	10.0	1.78	0.58
R1 891 CL	63.6	2.01	1.67
R3 891 CL	34.0	2.02	0.81
After pull-down			
S1 3131	4.4	1.83	0.73
S2 3131	3.6	1.80	0.09
S3 3131	4.8	2.00	0.14
S2 891	4.0	2.00	0.15
S3 891	16.4	1.57	0.61
R1 3131	7.2	2.00	0.17
R2 3131	4.4	1.83	0.52
R3 3131	10.0	1.66	0.55
R1 891	6.8	2.12	0.51
R2 891	6.4	2.00	0.72
R3 891	6.8	2.12	0.60
Control (non-transfected)			
S1 G5	73.2	2.01	1.28
S2 G5	49.6	2.00	1.67
S3 G5	48.8	2.00	0.75
R1 G5	149.0	1.87	1.46
R3 G5	230.0	2.00	1.62
R4 G5	79.6	1.97	2.11
R5 G5	190.0	2.01	1.98

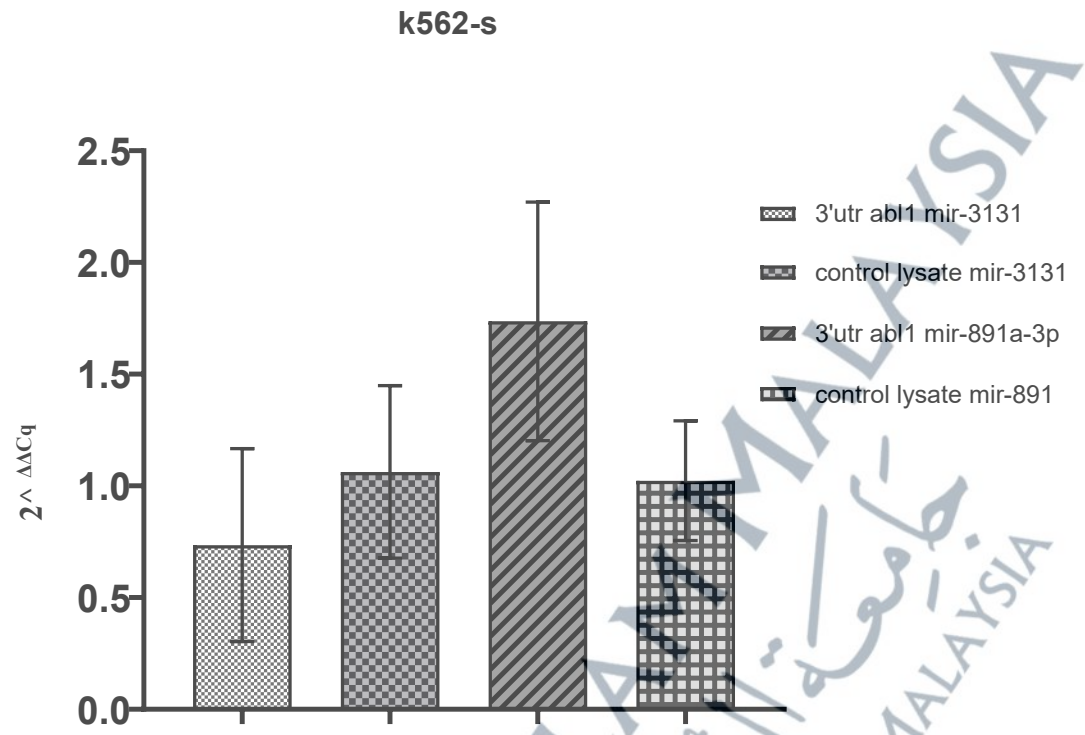

Figure 4.12: Hsa-miR-3131 and hsa-miR-891-3p target identification by qPCR compared to the control lysate in k562-s.

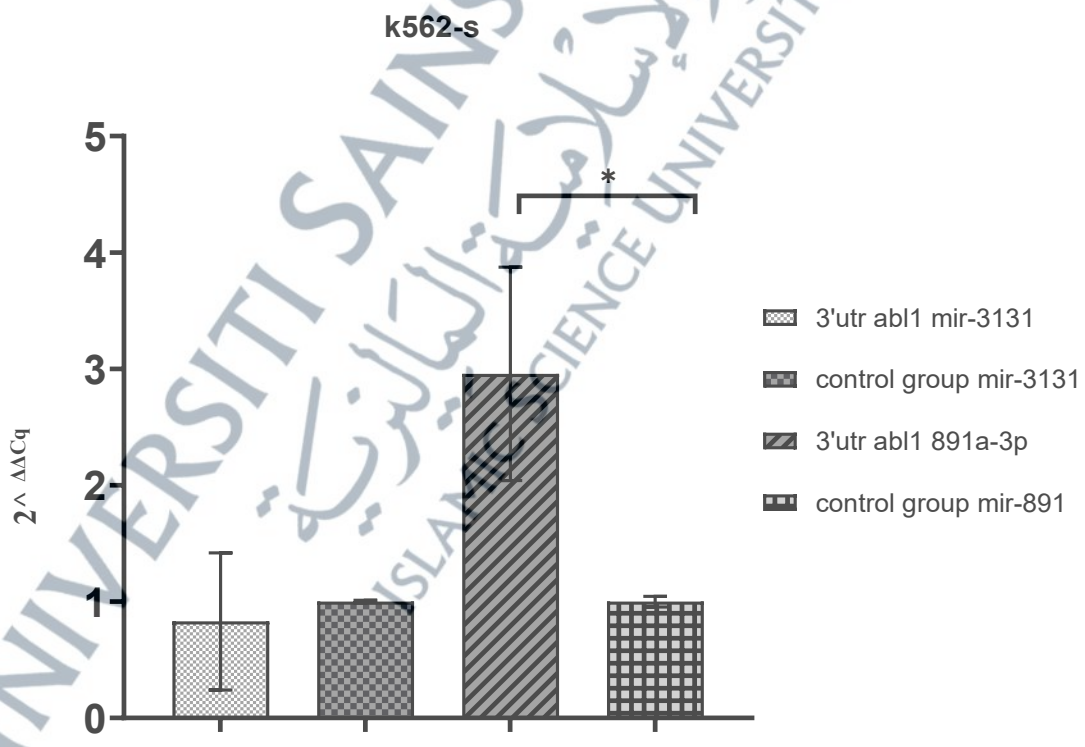

Figure 4.13: Hsa-miR-3131 and hsa-miR-891-3p target identification by qPCR compared to the control group in k562-s. * $p<0.05$.

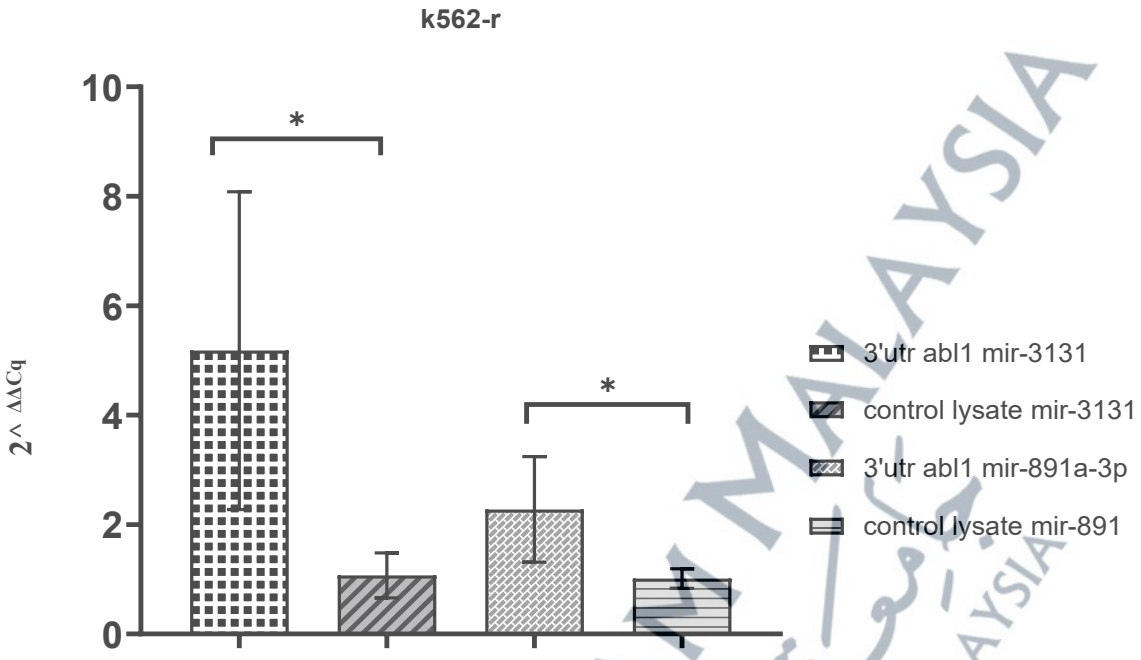

Figure 4.14: Hsa-miR-3131 and hsa-miR-891-3p target identification by qPCR compared to the control lysate in k-562-r. * $p<0.05$.

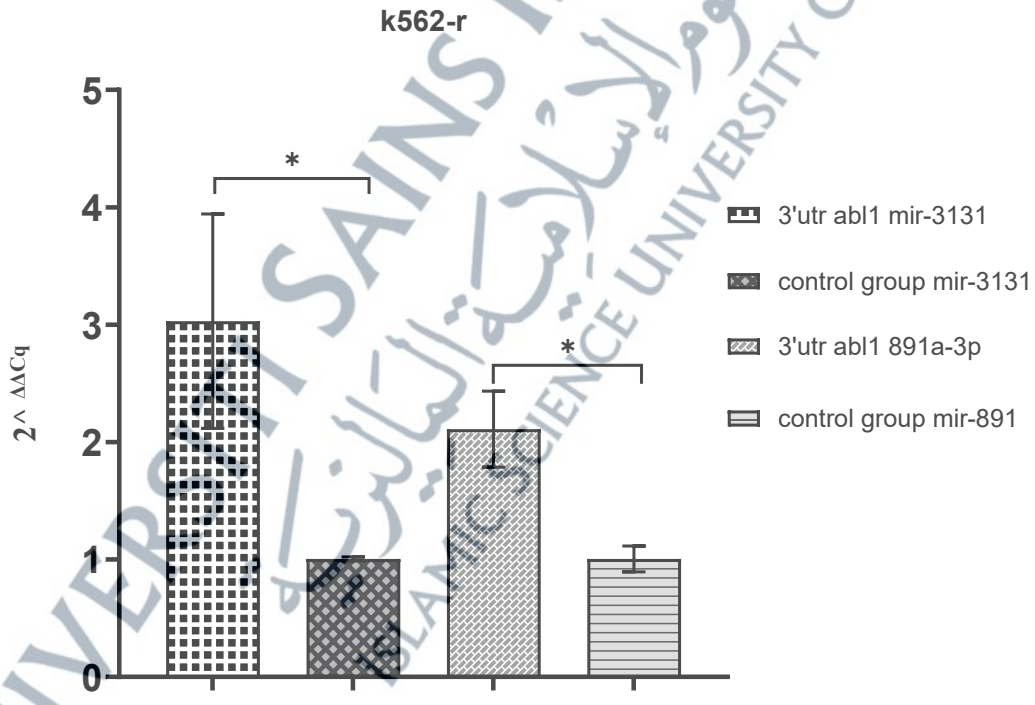

Figure 4.15: Hsa-miR-3131 and hsa-miR-891-3p target identification by qPCR compared to the control group in k562-r. *$p<0.05$.

4.3 *BCR-ABL1* and *ABL1* Expression

4.3.1 Housekeeping genes (HKG) selection

During the preliminary qPCR, it is necessary to choose the housekeeping genes to ensure reliable normalisation of target gene expression. From the listed housekeeping genes listed in Table 3.2, Cq results from each primer set were analysed using RefFinder (https://www.heartcure.com.au/reffinder/), a web-based comprehensive tool that calculated the geometric mean of the Cq for the overall final ranking. This tool summarised calculations done by Genorm, Bestkeeper, normFinder and Delta Ct method. These algorithms rank genes based on expression stability, which reflects how consistently a gene is expressed across all samples and experimental conditions. A lower variability in Cq values indicates greater stability. As shown in Figure 4.16, GAPDH displayed the lowest variation and highest stability score across all samples, followed by PGK1, ACTB and PP1B (least stable). Based on these criteria, GAPDH was selected as the reference gene for the *ABL1* and *BCR-ABL1* gene expression quantification. Figure 4.17 shows the stability ranking from each algorithm, and the average Cq values for each housekeeping gene are listed in Table 4.15.

Table 4.15: Average of Cq values from different groups.

Avg.Cq value	ACTB	GAPDH	PP1B	PGK1
K562-s G1	16.36	17.42	21.24	20.50
K562-s G2	18.36	18.78	21.96	21.54
K562-s G3	16.84	18.24	21.31	21.14
K562-s G4	15.89	16.81	20.68	19.27
K562-s G5	16.43	16.62	20.90	19.51

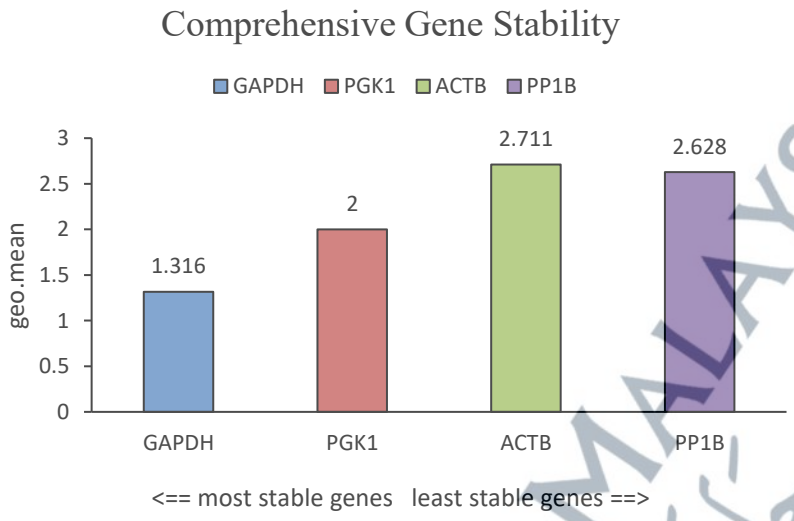

Figure 4.16: Summary of housekeeping genes stability.

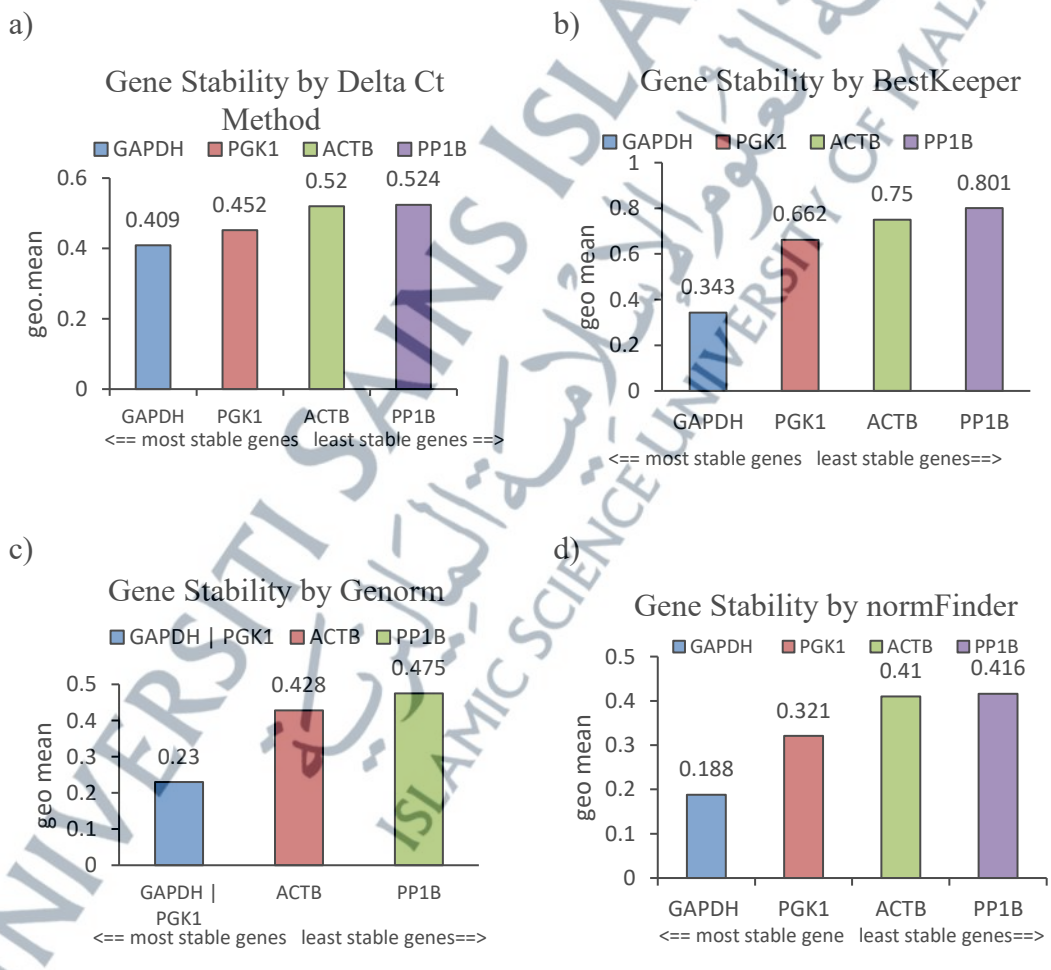

Figure 4.17: Gene stability from (a)Delta Ct method, b) BestKeeper, (c) Genorm, and (d) normFinder tools.

4.3.2 PCR efficiency determination

Primers listed in Table 3.2 were subjected to PCR efficiency determinations. Table 4.16 - 4.18 shows primer amplification and standard curves. The minimum and maximum requirements of the cDNA template were noted for subsequent experiments. All primers showed R^2 of more than 0.9 and efficiency between the 90-110% range using a 10-fold serial dilution of cDNA.

Table 4.16: PCR efficiency amplification and standard curves for selected primers.

Amplification curve	Standard curve
ABL1	R^2: 0.97, Eff%: 111.3
BCR-ABL1	R^2: 0.93, Eff%: 113.9

Table 4.17: PCR efficiency amplification and standard curves for selected primers (continued).

Amplification curve	Standard curve
Beta-actin	R^2: 0.96, Eff%: 108.7
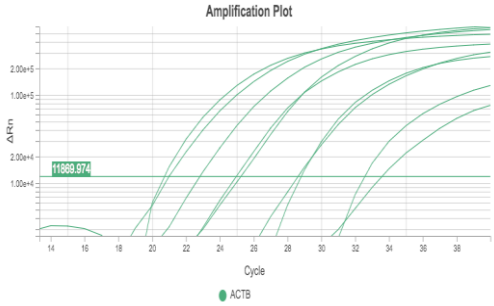	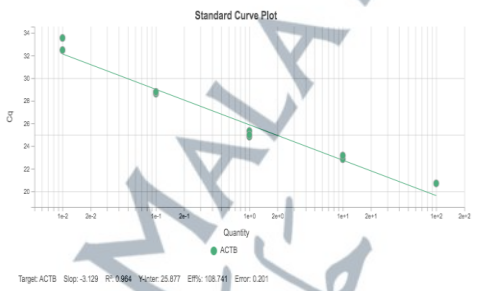
GAPDH	R^2: 0.95, Eff%: 108.8
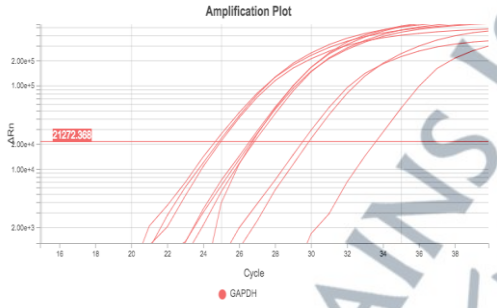	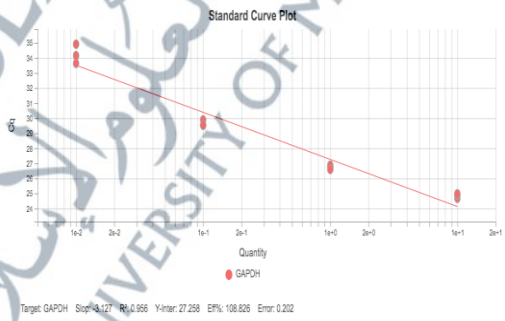
PGK1	R^2: 0.948, Eff%:94.3
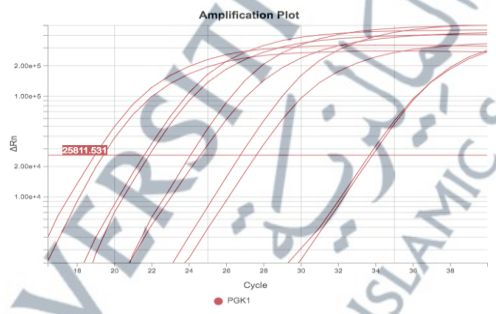	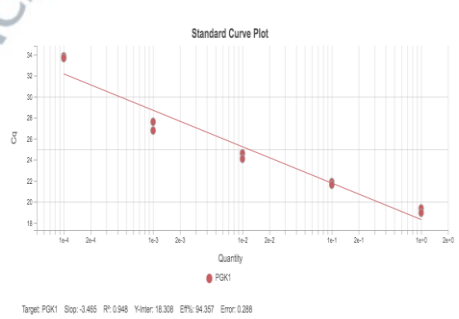

Table 4.18: PCR efficiency amplification and standard curves for selected primers (continued).

Amplification curve	Standard curve
PP1B	R^2: 0.997, Eff%: 111.9
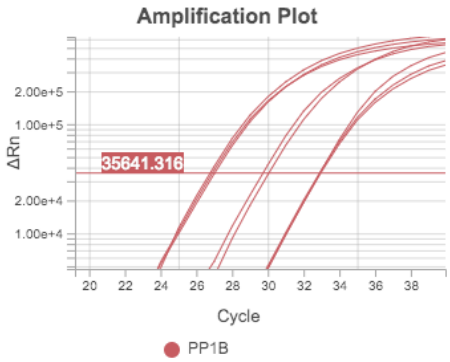	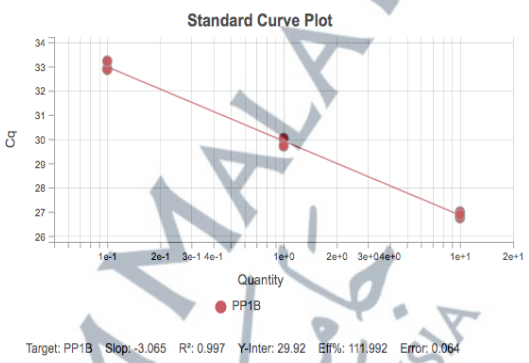

4.3.3 *ABL1* and *BCR-ABL1* gene expression

Figure 4.18 shows that, in K562-s cells, hsa-miR-3131 significantly reduced the expression of *ABL1* (0.737 ± 0.142) and *BCR-ABL1* (0.383 ± 0.194) compared to control group ($p< 0.05$). In k562-r cells (Figure 4.19), however, only *ABL1* expression was significantly decreased ($p<0.05$) following transfection with hsa-miR-3131 (0.607 ± 0.260), hsa-mir-891a-3p (0.500 ± 0.292), and osa-mir1858a/b (0.500 ± 0.085). These findings indicated that miRNA transfection affected gene expression in both cell types. Hsa-mir-3131 had the strongest suppressive effect on *ABL1* and *BCR-ABL1* expression in k562-s cells, whereas all three miRNAs showed greater impact on *ABL1* expression in K562-r cell. Notably, hsa-miR-3131 effectively suppressed *BCR-ABL1* expression only in k562-s cells. Furthermore, imatinib (IM) treatment led to increased gene expression in the K562-r group compared with both the untreated and miRNA-treated groups.

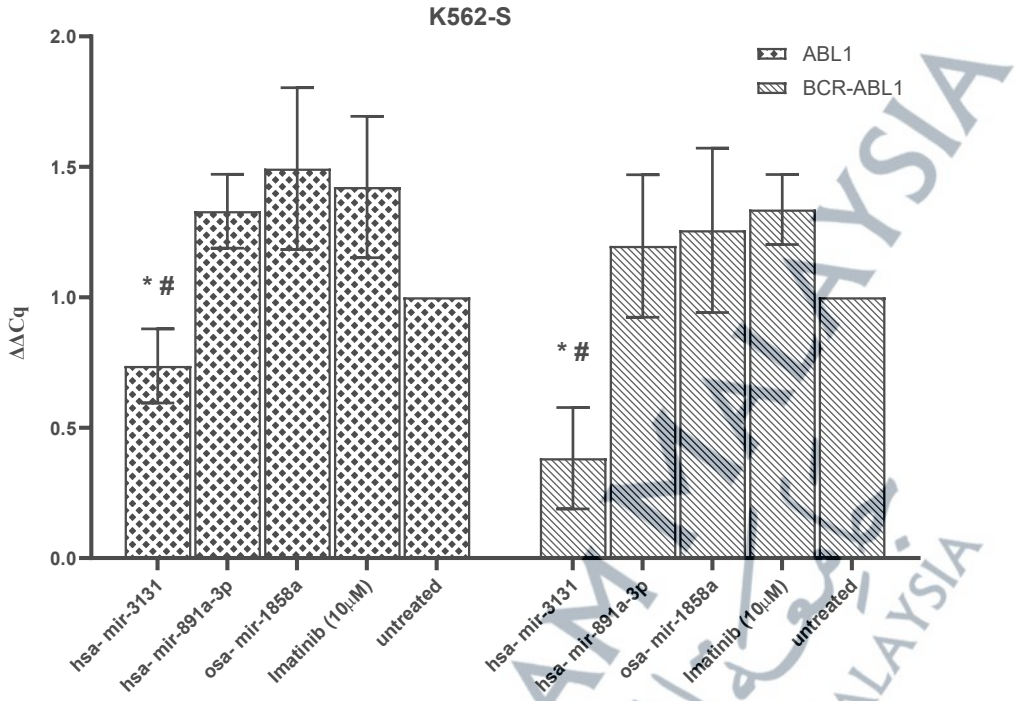

Figure 4.18: *ABL1* and *BCR-ABL1* gene expression in k562-s cells. The results were stated as mean ± SD (n = 3), * significant with $p<0.05$ compared to untreated, # significant with $p<0.05$ compared to imatinib.

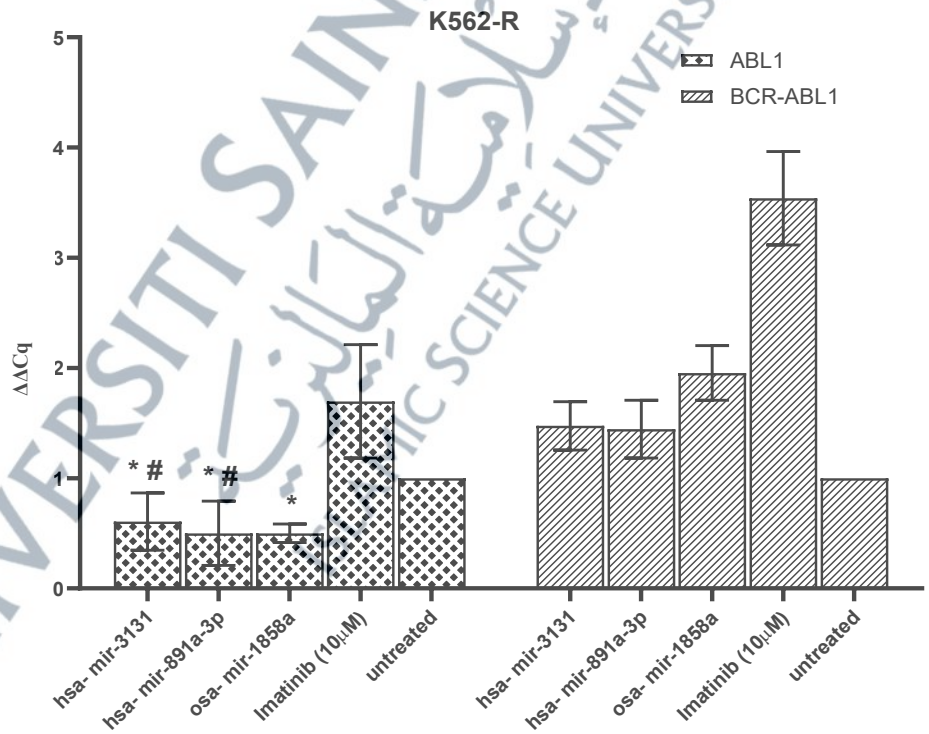

Figure 4.19: *ABL1* and *BCR-ABL1* gene expression in k562-r cells. The results were stated as mean ± SD (n = 3), * significant with $p<0.05$ compared to untreated, # significant with $p<0.05$ compared to imatinib.

4.4 ABL1 Protein Analysis of Cell-Based ELISA

The ABL1 protein concentration in cells was measured using the ABL1 (Human) Cell-Based ELISA Kit. The kit measured the relative amount of ABL1 in cultured cells and qualitatively determined the target protein concentration by an indirect ELISA format. Following the colourimetric measurement of HRP activity via substrate addition, the crystal violet whole-cell staining method was used to normalise the absorbance values to cell counts. Figure 4.20 indicates lower ABL1 protein expression in k562-s cells transfected with all three miRNAs compared to imatinib with $p<0.05$. However, there were no significant differences in ABL1 protein concentration between treated and untreated groups in k562-s cells. Meanwhile, ABL1 protein concentration in k562-r cells transfected with osa-miR1858a/b (1.787 ± 0.08) was significantly higher than imatinib (0.973 ± 0.22) ($p<0.05$). ABL1 protein concentration in hsa-miR-3131 (1.207 ± 0.16) and hsa-miR-891a-3p (1.270 ± 0.35) were lower than untreated groups (1.540 ± 0.36) (Figure 4.21). However, these were not significant.

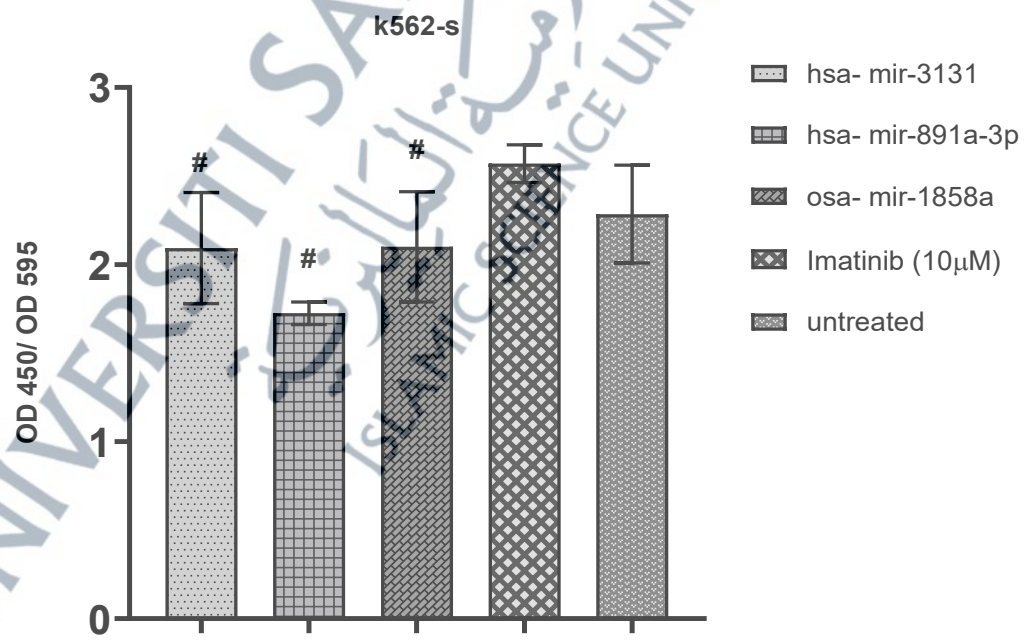

Figure 4.20: ABL1 protein expressions in k562-s. # $p<0.05$ compared to imatinib. Data are presented as mean ± SD from three biological replicates.

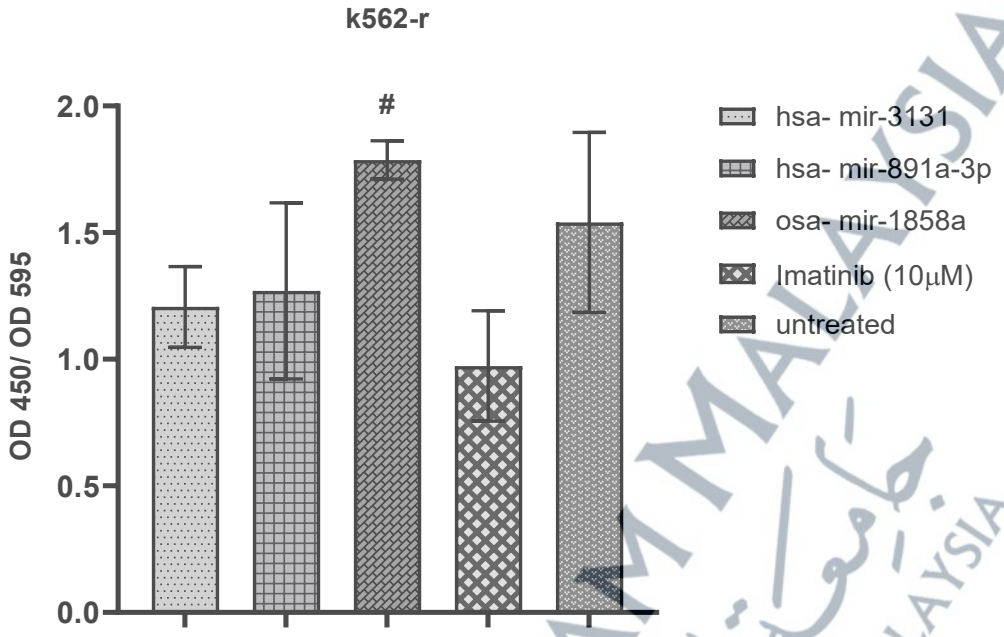

Figure 4.21: ABL1 protein expression in k562-r. # $p<0.05$ compared to imatinib. Data are presented as mean ± SD from three biological replicates.

4.5 Determination of Cell Functional Assay

4.5.1 Cell proliferation using MTS assay

Cell proliferation was found to be reduced in cells transfected with hsa-miR-3131, hsa-miR-891a-3p and osa-miR-1858a/b mimics after 48 hours incubation compared to untreated in both cells ($p<0.05$). Results show that cell proliferation reduction was most noticeable with osa-miR-1858a/b transfection in k562-r cell with 50.5% ± 1.53 compared to untreated ($p<0.05$). However, k562-s cell viability was only reduced to 84.45 % ± 0.673 (hsa-miR-3131), 81.45 % ± 0.816 (miR-891a-3p) and 83.86 % ± 0.733 (osa-miR1858a/b) with $p<0.05$ compared to untreated (Figure 4.22). Meanwhile, the imatinib (10 μM) treated group displayed the lowest cell proliferation rate in both cells, with 7.7% ± 0.19 in k562-s and 41.8% ± 1.61 in k562-r cells.

Cell proliferation in K562-r (imatinib-resistant) cells was only slightly reduced following imatinib treatment, as expected for resistant cells. These findings revealed that miRNA transfection successfully inhibited cell proliferation in both K562-s and K562-r cells. The most significant reduction was observed for osa-miR1858a/b in k562-r, where cell viability dropped by about 50% compared to untreated cells ($p<0.05$). This suggests that miRNA may play a role in modulating resistance mechanism in cancer cells.

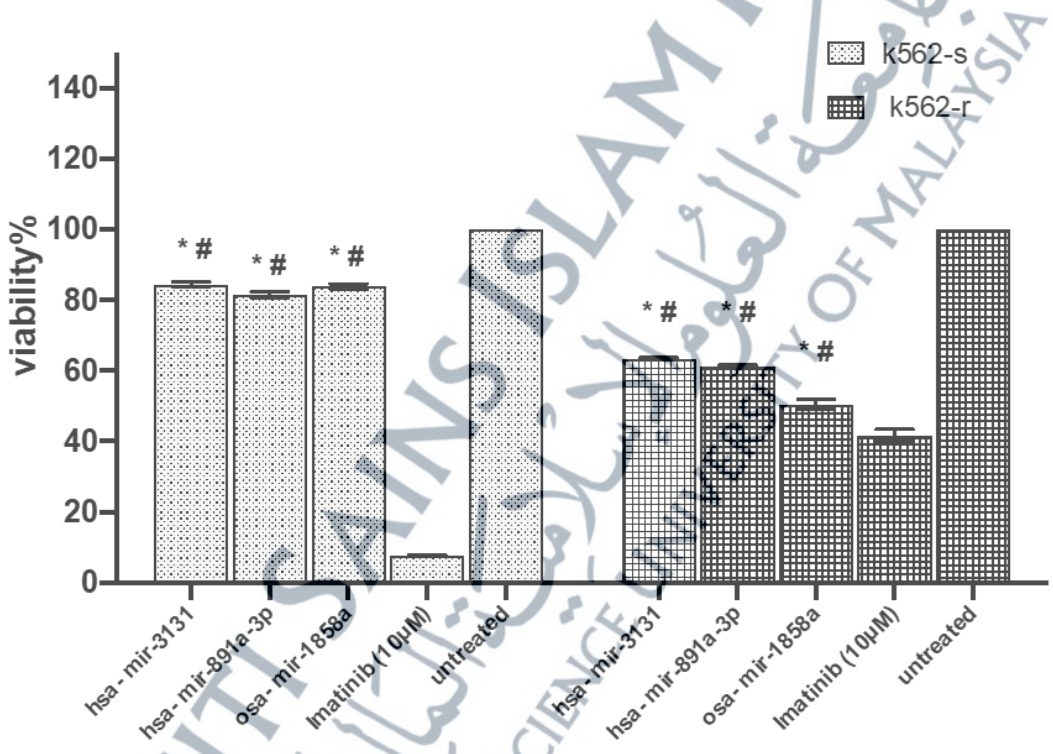

Figure 4.22: k562-s and k562-r cells viability post-transfection with miRNA mimics. The results were stated as mean ± SD with three biological replicates, * significant with $p<0.05$ compared to untreated, # significant with $p<0.05$ compared to imatinib.

4.5.2 Flow cytometry analysis of cell cycle

Figure 4.23 showed that K562-s cells transfected with osa-miR-1858a/b induced a cell cycle arrest at the S phase compared to untreated with 59.74% ± 1.34 and 55.80% ± 2.35, respectively ($p<0.05$). Osa-miR1858a/b also induced a cell cycle arrest at the

G2/M phase compared to untreated ($p<0.01$). Meanwhile, imatinib was found to induce the cell cycle arrest during the G0/G1 phase with 81.73% ± 2.53 and 78.8% ± 5.1 compared to other groups ($p<0.05$) in k562-s and k562-r respectively (Figure 4.23 and Figure 4.24). Moreover, the G2/M phase of hsa-miR-891a-3p and osa-miR-1858a/b transfected groups were shown to induce a cell cycle arrest with 8.6% ± 1.1 and 6.5% ± 0.9 respectively, ($p< 0.05$) compared to untreated 4.7% ± 0.6 (Figure 4.24) in the k562-r cell.

Tables 4.19 and 4.20 showed a cell cycle phase in the population histogram and PI-W versus PI-A scatter plot. Generally, it can be assumed that osa-miR-1858a/b induced a cell cycle arrest in k562-s cells at the S phase and G2/M phase ($p<0.05$). Meanwhile, hsa-miR-891a-3p and osa-miR-1858a/b displayed a higher percentage of cell cycle arrest at G2/M in k562-r than untreated. Meanwhile, hsa-mir-3131 was significantly higher at the S and G2/M phases than imatinib in both cell types ($p<0.05$).

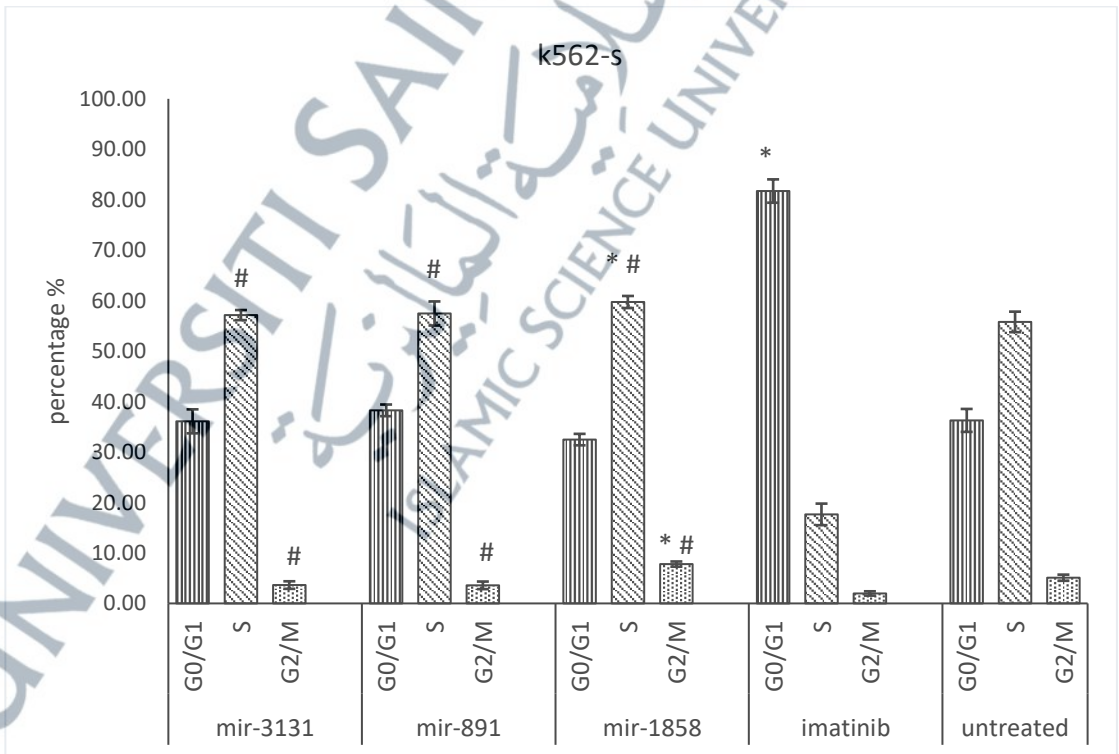

Figure 4.23: Effects of miRNA transfection in k562-s cell cycle was plotted in cell cycle percentage (%). Data expressed in mean ± SD from three biological replicates. * p<0.05 compared to untreated, # p<0.05 compared to imatinib.

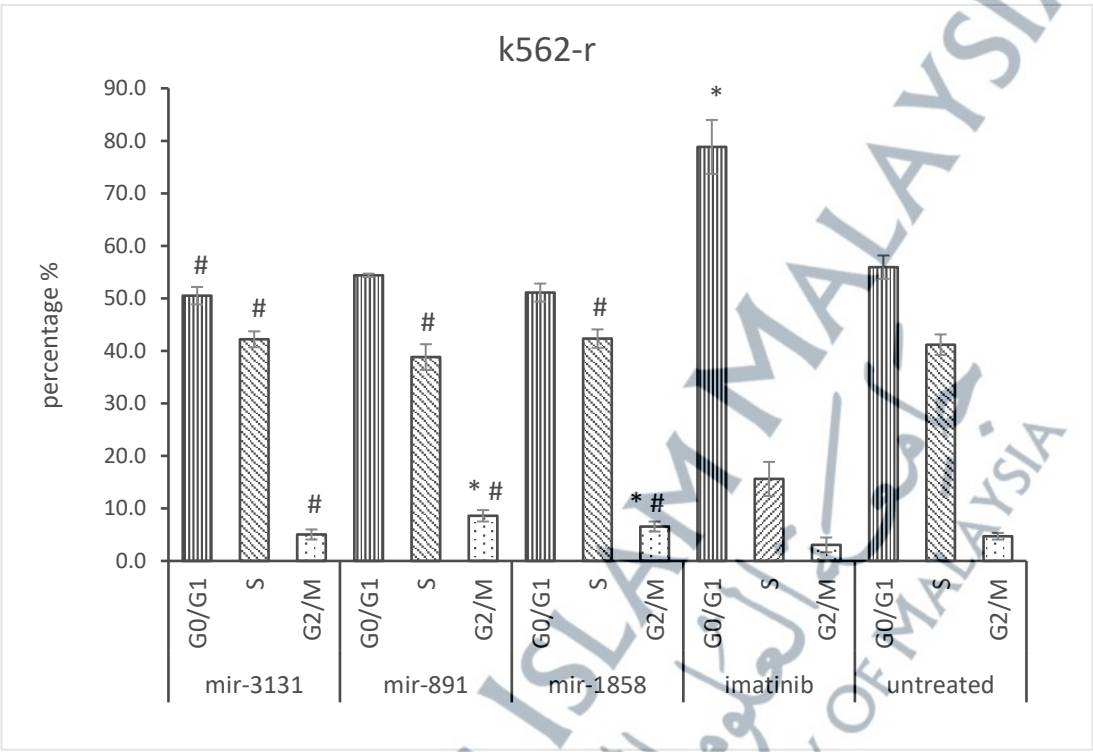

Figure 4.24: Effects of miRNA transfection in the k562-r cell cycle were plotted in cell cycle percentage (%). Data expressed in mean ± SD from three biological replicates. * p<0.05 compared to untreated, #p<0.05 compared to imatinib.

Table 4.19: k562-s cell cycle shown in population histogram (a, b, c, d, e), in scatter plot of PI-W versus PI-A(f, g, h, i, j) and percentage (%).

k562-s	Hsa-miR-3131	Hsa-miR-891a-3p	Osa-miR-1858a/b	Imatinib (10μM)	Control (untreated)
	a) 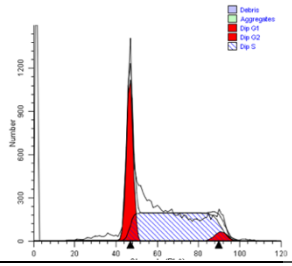	b) 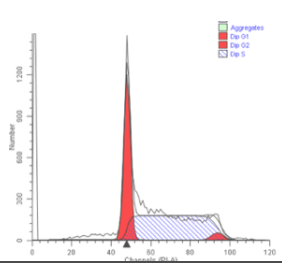	c) 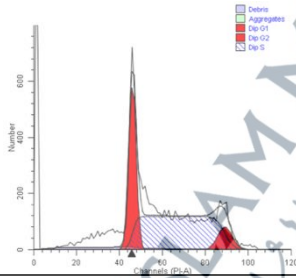	d) 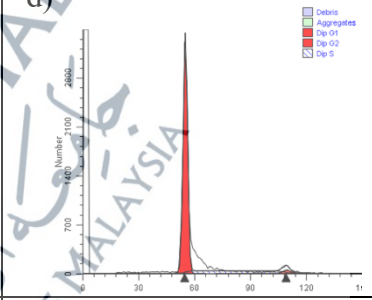	e) 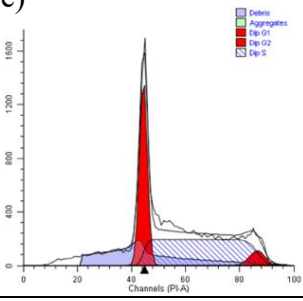
	f) 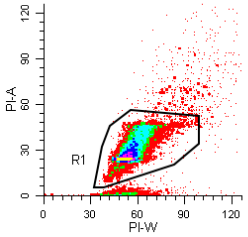	g) 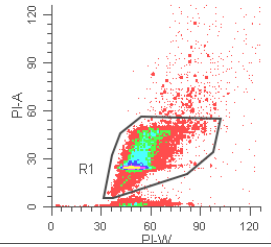	h) 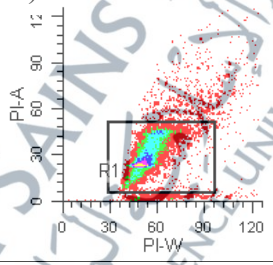	i) 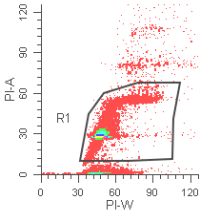	j) 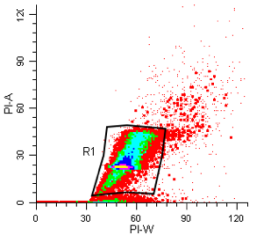
G0/G1(%)	36.10 ± 2.57	38.26 ± 1.33	32.47 ± 1.27	81.73 ± 2.53	36.27 ± 2.54
S (%)	57.14 ± 1.15	57.47 ± 2.76	59.74 ± 1.34	17.64 ± 2.40	55.80 ± 2.35
G2/M (%)	3.64 ± 0.84	3.59 ± 0.92	7.80 ± 0.58	1.98 ± 0.50	5.01 ± 0.68

Table 4.20: k562-r cell cycle shown in population histogram (a, b, c, d, e), scatter plot of PI-W versus PI-A (f, g, h, i, j) and percentage (%).

k562-r	Hsa-miR-3131	Hsa-miR-891a-3p	Osa-miR-1858a/b	Imatinib (10µM)	Control (untreated)
	a) 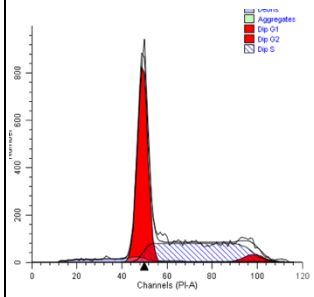	b) 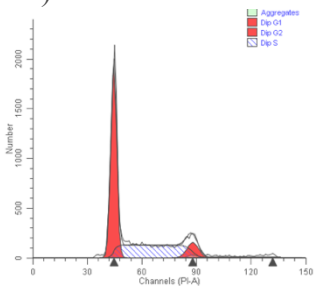	c) 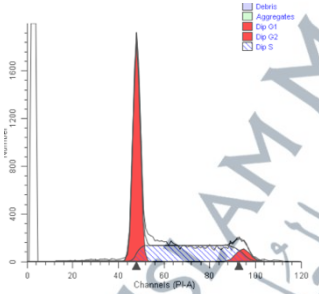	d) 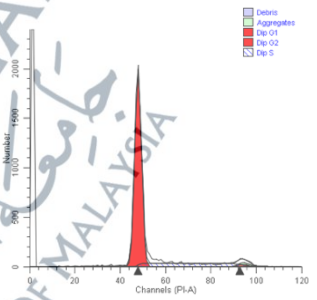	e) 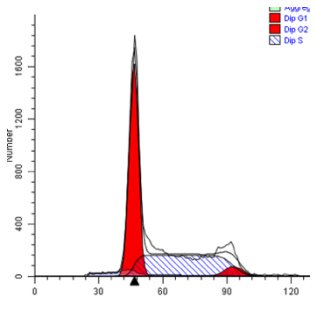
	f) 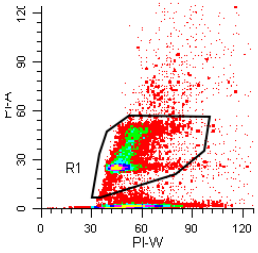	g) 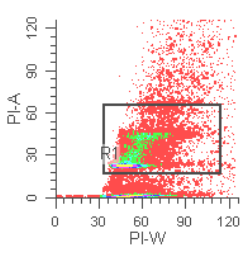	h) 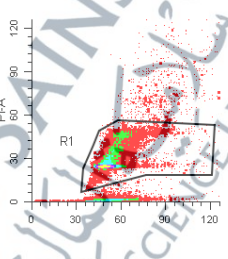	i) 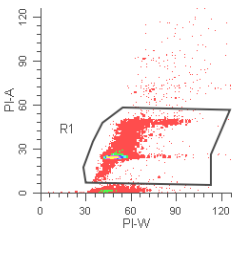	j) 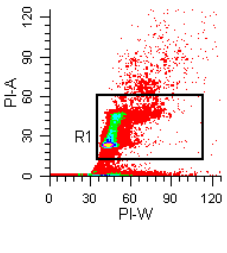
G0/G1 (%)	50.5 ± 1.7	54.4 ± 0.3	51.1 ± 1.7	78.8 ± 5.1	55.9 ± 2.2
S (%)	42.2 ± 1.5	38.8 ± 2.5	42.3 ± 1.7	15.6 ± 3.2	41.2 ± 2.0
G2/M (%)	5.0 ± 1.0	8.6 ± 1.1	6.5 ± 0.9	3.1 ± 1.4n	4.7 ± 0.6

4.6 Microarray Profiling

4.6.1 RNA quality

Extracted RNAs were sent to quality control before microarray using Agilent 2100 Bioanalyzer of the Eukaryote Total RNA Nano assay version 2 (Agilent Technologies, United States). Figures 4.25 and 4.26 show the electrophoresis diagram of k562-s and k562-r of different samples. From these, two samples did not pass RIN, the S48 NOR (2) and R48 NOR (2). These samples were not used in microarray analysis. Table 4.21 shows the RNA integrity number (RIN) and concentration of each sample.

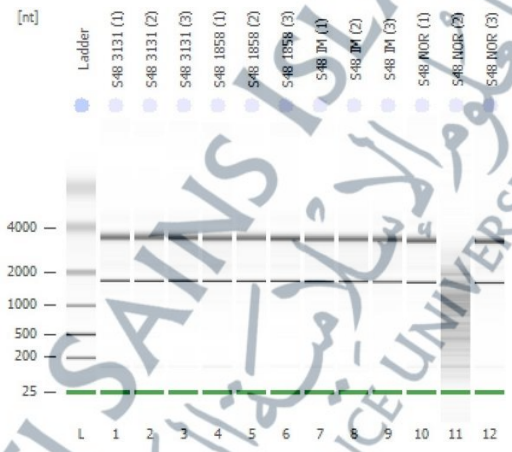

Figure 4.25: Electrophoresis file run summary of RNA extracted from k562-s cells treated with hsa-miR-3131, osa-miR1858a/b, imatinib and untreated (normal) in triplicate.

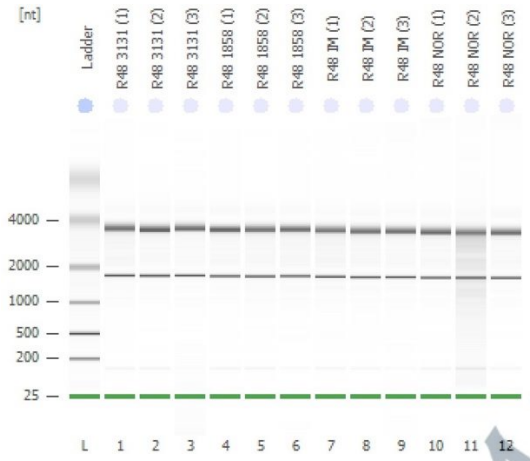

Figure 4.26: Electrophoresis file run summary of RNA extracted from k562-r cells treated with hsa-miR-3131, osa-miR1858a/b, imatinib and untreated (normal) in triplicate.

Table 4.21: RNA integrity number (RIN) and concentration (ng/ml) from each sample sent for quality control before microarray.

Sample Name	RNA integrity number (RIN)	RNA concentration (ng/µl)
S48 3131 (1)	9.80	377
S48 3131 (2)	9.90	124
S48 3131 (3)	9.80	109
S48 1858 (1)	9.60	403
S48 1858 (2)	9.90	110
S48 1858 (3)	9.90	141
S48 IM (1)	9.80	234
S48 IM (2)	9.80	52
S48 IM (3)	9.90	54
S48 NOR (1)	9.90	303
S48 NOR (2)	3.50	94
S48 NOR (3)	9.70	98
R48 3131 (1)	9.60	273
R48 3131 (2)	9.80	282
R48 3131 (3)	10	45
R48 1858 (1)	9.80	295
R48 1858 (2)	9.60	310
R48 1858 (3)	9.80	128
R48 IM (1)	9.50	212
R48 IM (2)	9.70	201
R48 IM (3)	9.90	98
R48 NOR (1)	9.80	239
R48 NOR (2)	7.90	366
R48 NOR (3)	9.90	411

4.6.2 Microarray gene expression

Groups analysed by microarray included:(1) hsa-miR-3131, (2) osa-miR1858a/b, (3) imatinib, and (4) untreated cells each in biological duplicates. The microarray results showed no statistically significant differential expression genes (DEGs) between the miRNA transfected groups in either cell lines. Therefore, genes with fold change (FC) >2 were manually extracted from the original dataset (Appendix 2). These upregulated and downregulated genes were then submitted to the Database for Annotation, Visualization, and Integrated Discovery (DAVID) for the functional annotation, pathway analysis and gene ontology (GO) identification.

The resulting gene list from each group were merged and screened to find duplicates across datasets. These duplicate genes were re-analysed in DAVID to confirm the GO and pathways. Candidate genes for further validation were selected based on their association with pathways and biological process (BP) relevant to this study, including the MAPK cascade, positive regulation of cell proliferation, hematopoietic cell lineage, MAPK signalling pathway, PI3K-Akt signalling pathway and positive regulation of G1/S transition of mitotic cell cycle.

Before proceeding with qPCR validation, each selected candidate gene's expression was checked in the NCBI database to confirm its presence in the bone marrow. Genes with confirmed expression in bone marrow, as indicated by NCBI expression profiles, were prioritised for further analysis. Table 4.22 presents the selected pathways of each comparison group and Table 4.23 lists the selected genes and their corresponding expression status.

Table 4.22: Summary of selected biological processes and pathways related to the study.

Groups	Category	Term	Genes	p-value
S3131 vs SNOR	i) Goterm_Bp_Direct ii) Kegg_Pathway iii) Goterm_Bp_Direct	GO:0000165~MAPK cascade ii) Hsa04010: MAPK signalling pathway iii) GO:0043410~positive regulation of MAPK cascade	i) RET, **MYC**, TNF, RASGRP3 ii) MYC, TNF, RASGRP3 iii) RET, **TNF**	2.84E-06 0.012 0.041

Groups	Category	Term	Genes	p-value
S1858 vs SNOR	i) Kegg_Pathway ii) Goterm_Bp_Direct iii) Kegg_Pathway	i) hsa04151: PI3K-Akt signalling pathway ii) GO:0008284~positive regulation of cell proliferation iii) hsa04010: MAPK signalling pathway	i) CDKN1A, CSF3R, **CSF1**, EGF, PDGFB, FN1, LAMB1, IGF1, GNG12, FGF5, **IL6**, FGF8, GNG4, BCL2, GNB3, MET, FGFR1 ii) FGF5, IL6, FGF8, THPO, CSF1, EGF, TRAF5, PDGFB, BCL2, FN1, IGF1, FGFR1 iii) FGF5, FGF8, GADD45B, CSF1, EGF, PDGFB, IGF1, GNG12, TNF, MET, FGFR1	9.33E-16 7.90E-11 1.56E-08
R3131 vs RNOR	i) Goterm_Bp_Direct ii) Goterm_Bp_Direct iii) Kegg_Pathway iv) Goterm_Bp_Direct	i) GO:0008284~positive regulation of cell proliferation ii) GO:0000165~MAPK cascade iii) hsa04640: Hematopoietic cell lineage iv) GO:1900087~positive regulation of G1/S transition of mitotic cell cycle	i) CSF2, IL1B, PROK2, AIF1 ii) CCL5**, IL1B**, CCL3 iii) IL1A, CSF2, IL1B iv) **TERT**, PLCB1, AIF1	0.003 0.002 0.003 3.73E-04

R1858 vs RNOR	i) Kegg_Pathway ii) Goterm_Bp_Direct iii) Kegg_Pathway	i) Hsa04010: MAPK signalling pathway ii) GO:0008284~positive regulation of cell proliferation iii) hsa04151: PI3K-Akt signalling pathway	i) **MAP4K1**, FGF5, PAK1, ERBB2, FGF3, FGF10 ii) FGF5, **PAK1,** ERBB2, FGF3, FGF10 iii) FGF5, IL2RA, ERBB2, FGF3, FGF10	2.27E-05 1.84E-04 9.03E-04

*Selected genes were highlighted in bold

Table 4.23: Selected genes for qPCR validation.

Gene official symbol	Official full name	Status
IL6	Interleukin-6	downregulated
MYC	Myc proto-oncogene protein	downregulated
MAP4K1	Mitogen-activated protein kinase kinase kinase kinase 1	downregulated
PAK1	Serine/threonine-protein kinase PAK 1	downregulated
TERT	telomerase reverse transcriptase	downregulated
IL1B	interleukin 1 beta	Upregulated
TNF	TNF tumor necrosis factor	Upregulated
CSF1	Macrophage colony-stimulating factor 1	Upregulated

4.6.3 PCR efficiency determination of selected genes

All primers in Table 3.3 were subjected to PCR efficiency determination. Standard curves were constructed with minimum and maximum requirements of the cDNA template and were noted for subsequent experiments. Table 4.24 – 4.26 displays the amplification and standard curve for each primer set.

Table 4.24: PCR efficiency amplification and standard curves for selected primers.

Amplification curve	Standard curve
IL6	R^2:0.99, Eff%: 106.4
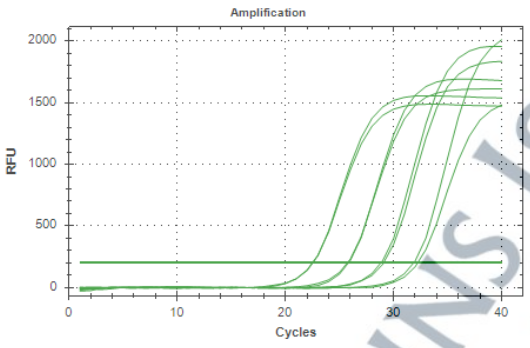	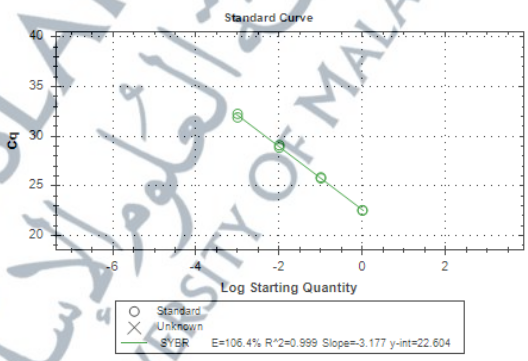
CSF1	R^2: 0.995, Eff%: 108.6
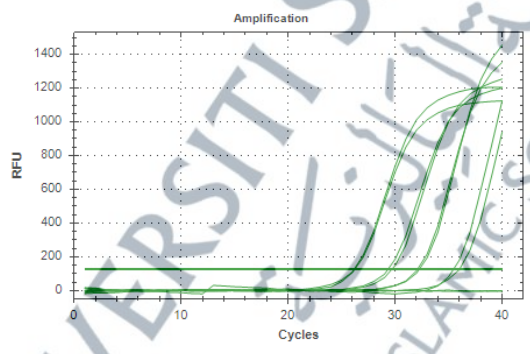	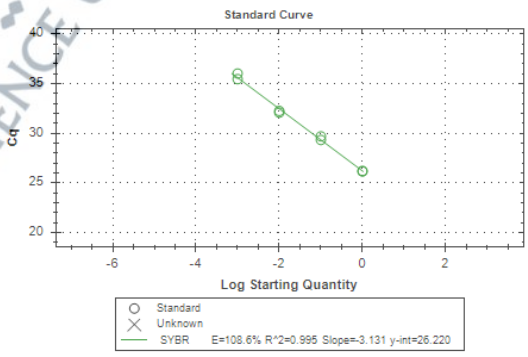

Table 4.25: PCR efficiency amplification and standard curves for selected primers (continued).

Amplification curve	Standard curve
TNF1	R^2: 0.994, Eff%: 108.1
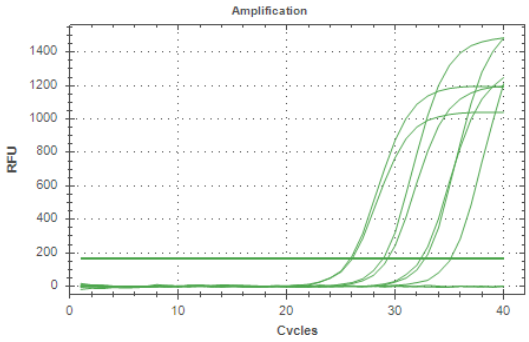	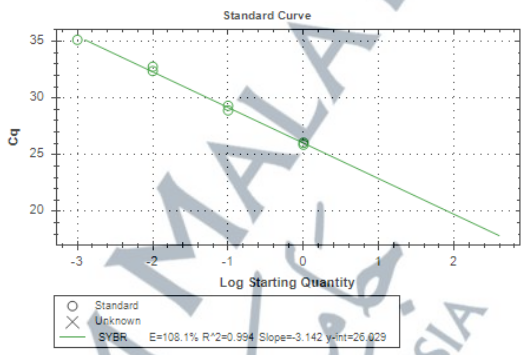
MAP4K1	R^2: 0.996, Eff%: 110.5
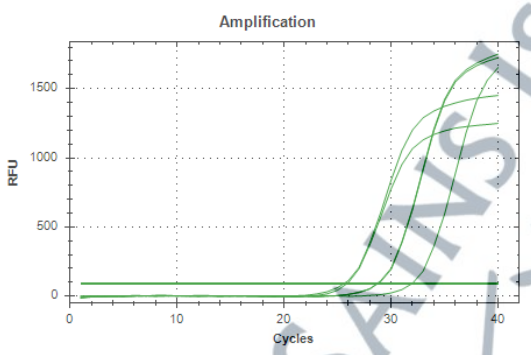	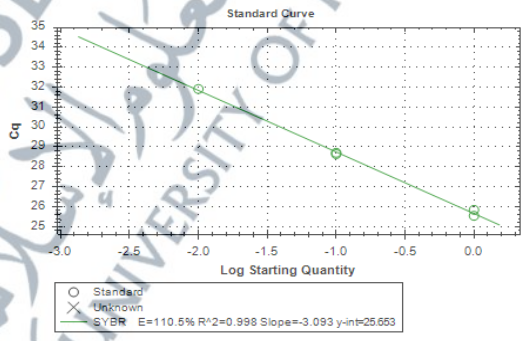
IL1B	R^2:0.997, Eff%: 97.2
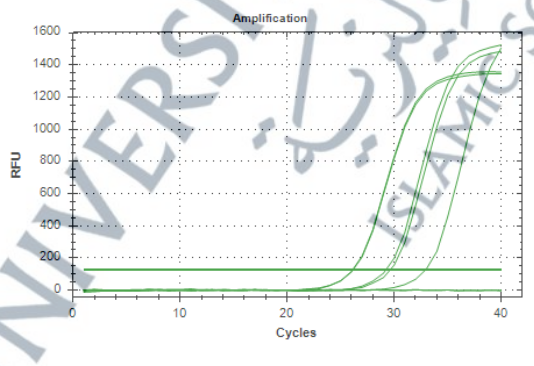	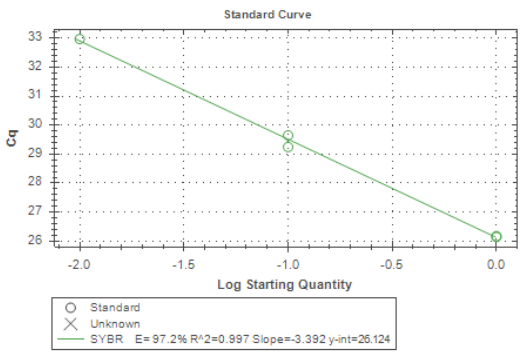

Table 4.26: PCR efficiency amplification and standard curves for selected primers (continued).

Amplification curve	Standard curve
MYC	R^2:0.999, Eff%: 100.3
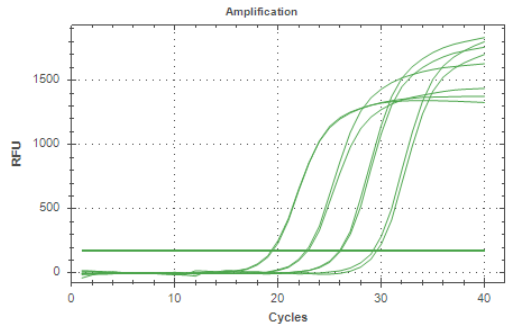	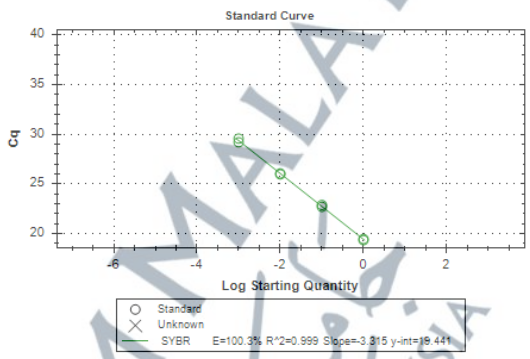
PAK1	R^2: 0.998, Eff%: 97.8
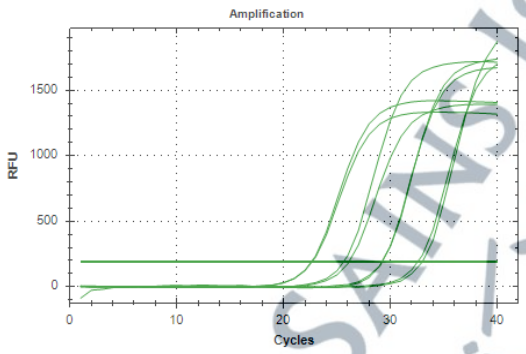	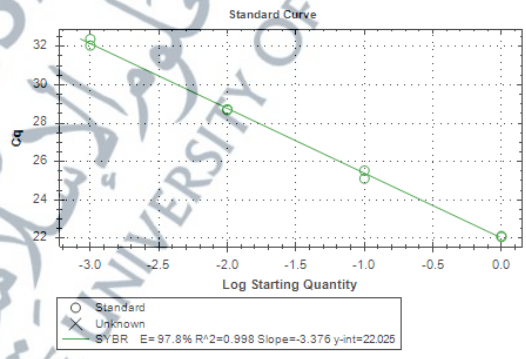
TERT	R^2: 0.981, Eff%: 101.2
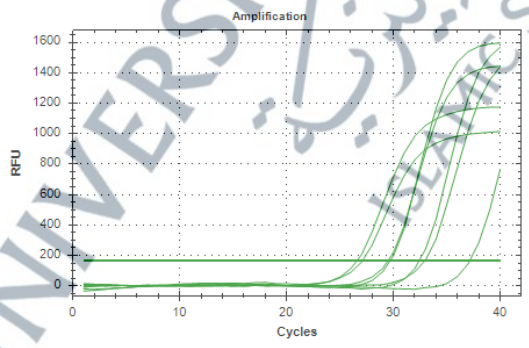	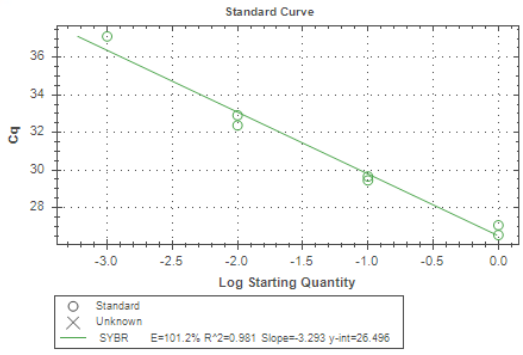

4.6.4 qPCR validation of up and down-regulated genes

Following several evaluations of gene ontology (GO) and pathways, the genes chosen for validation in quantitative polymerase chain reaction (qPCR) were MYC, TNF, CSF1, and IL6 in the k562-s cell line, whereas IL1B, TERT, MAP4K1, and PAK1 were selected for validation in the k562-r cell line. Figure 4.27 reveals a significant difference in IL6 (-0.264 ± 0.18), CSF1 (2.804 ± 0.15), and TNF (6.962 ± 1.20) expression between the miRNA-treated and control untreated groups of k562-s ($p<0.05$). Moreover, Figure 4.28 shows a statistical difference in gene expression of MAP4K1 (-0.738 ± 0.13) and IL1B (5.029 ± 0.23) between the miRNA-treated groups and the control group of k562-r ($p<0.05$). Additionally, Figure 4.29 shows the overall qPCR gene expression validation. Furthermore, a comparison of expression between microarray and qPCR data was shown in Figure 4.30, and among all eight genes, only MYC expression was not parallel with microarray. The primer sequences used in qPCR are listed in Table 3.4. The primer design and validation for each gene's is displayed in Appendix 3.

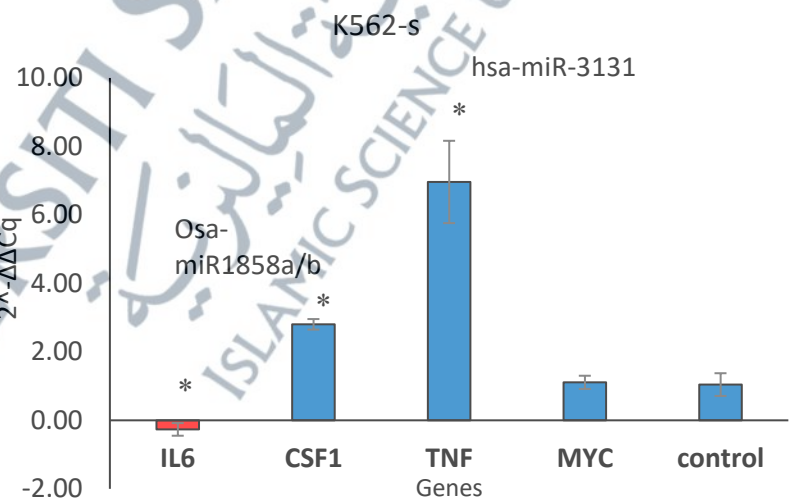

Figure 4.27: Gene expression from miR-3131 and osa-miR1858a/b treated groups compared to control untreated group in k562-s, * $p<0.05$.

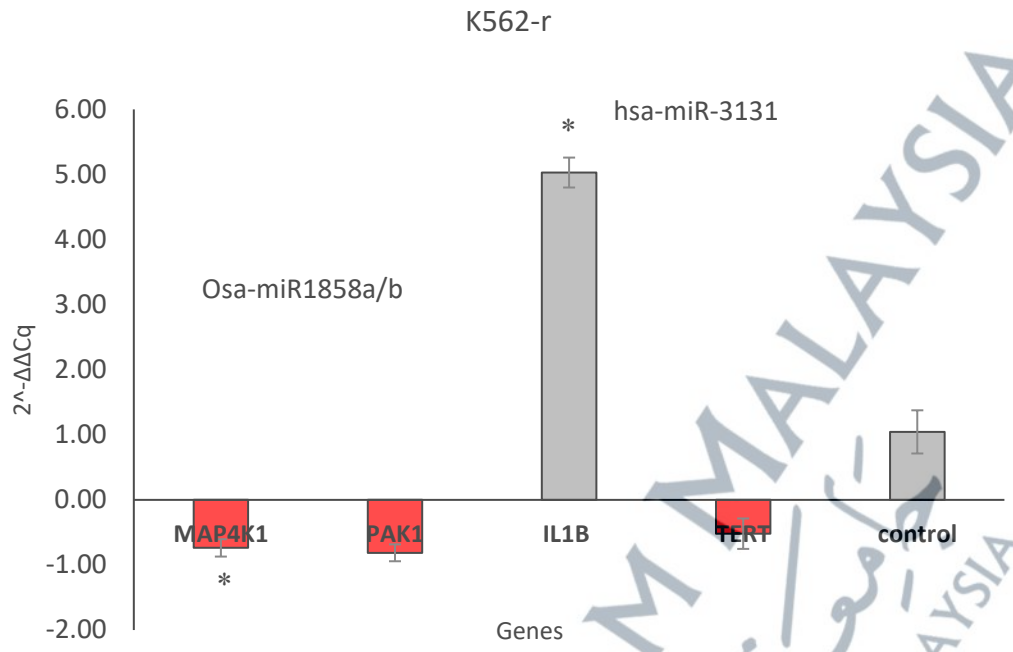

Figure 4.28: Gene expression from hsa-miR-3131 and osa-miR1858a/b treated groups compared to control untreated group in k562-r, *p<0.05.

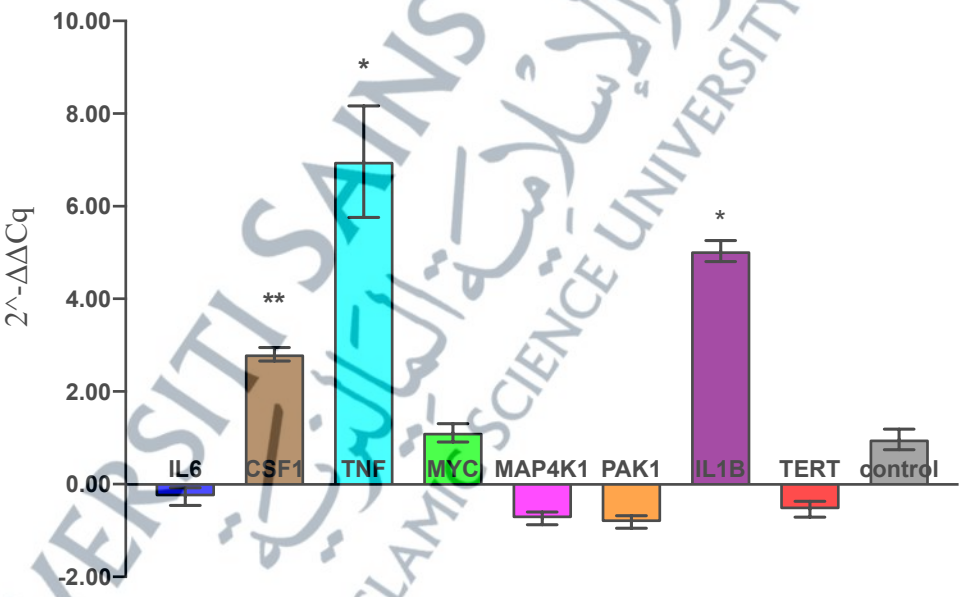

Figure 4.29: Overall gene expression from all miRNAs treated groups compared to the untreated control group. * p<0.05

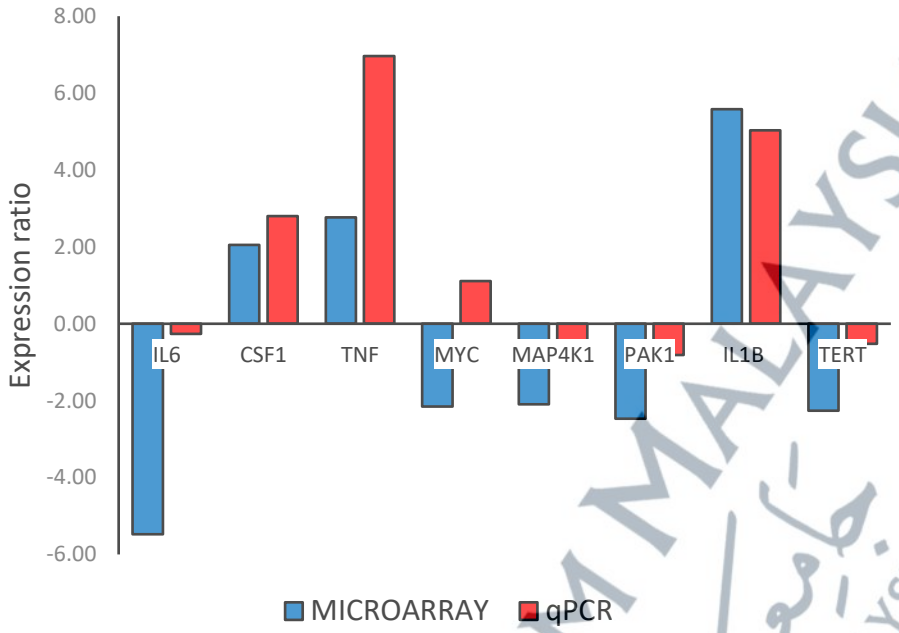

Figure 4.30: Gene expression comparison between microarray and qPCR.

4.6.5 Enrichment and pathway analysis of microarray genes

All the genes from microarray data were further subjected to in silico analysis for comparison with the results in subchapter 4.1.2. Figure 4.31 shows that the upregulated genes from the hsa-mir-3131 treated group in K562-s yield 12 clusters, but only three clusters (2, 3 and 6) produced functional enrichment results. Cluster 2 highlights G2/M checkpoints and DNA double-strand break repair involving H2BC1, ATM, PSMF1 and CHEK2 genes. In cluster 3, the TNF and MME genes were involved in a hematopoietic cell lineage pathway, while cluster 6 was associated with ABC transporter KEGG pathways involving ABCB6 and ABCC3 genes. Moreover, seven clusters were identified for the downregulated genes within the same group (Figure 4.32). Cluster 1 is specifically associated with the biological process of cell-cell adhesion, which occurs at the extracellular portion of the cell. This cluster is also implicated in important KEGG pathways, including PI3K-Akt and JAK-STAT, with the participation of IL2 and JAK1 genes.

Moreover, Figure 4.33 shows the upregulated genes that from osa-mir1858a/b treated group in k562-s cells were divided into 17 clusters. Out of these clusters, four clusters (clusters 1, 2, 3, and 13) were subjected to functional enrichment analysis. Proteins in cluster 1 are identified to be localised within the nucleus. Cluster 2 is associated with Ras, MAPK, and PI3K-Akt signalling pathways. It consists of FGF5, FGF8, CSF1, and PDGFB genes. Proteins in Cluster 3 are found in the cytoplasm and vesicles and play a role in cancer-related pathways. Cluster 13 is associated with the biological process and KEGG pathways of Wnt signalling, specifically including the genes DAAM2, RYK, and PRICKLE2.

Moreover, Figure 4.34 revealed that downregulated genes belonging to the same groups, resulted in the formation of 16 protein clusters. Cluster 1 encompasses proteins that regulate cell population proliferation, cell cycle, apoptosis, and hemopoiesis with the involvement of BCL2, BCL6, and IL10. This cluster is additionally linked to KEGG pathways such as pathways in cancer, FoxO, PI3K-Akt, p53, and JAK-STAT. Furthermore, proteins in cluster 2 are linked to cancer-related pathways, including the Ras and PI3K-Akt signalling pathways, encompassing GNB3, GNG12, and GNG4. Cluster 3 exhibits similar pathways to those previously found, including the PI3K-Akt pathway and cancer-associated route. However, it is worth noting that distinct genes, such as MET and IL6, are involved in these pathways. Proteins in cluster 4 were found in the cellular component of the external side of the plasma membrane, cell surface, plasma membrane, and intrinsic component of the membrane. These proteins are implicated in the JAK-STAT signalling pathway with IL21R and CSF3R genes. Finally, in cluster 6 of the same group, most proteins are engaged in the MAPK signalling pathway and apoptosis, specifically with the presence of GADD45B and DDIT3.

Nevertheless, transfecting K562-r cells with hsa-miR-3131 results in the upregulation of genes, leading to the formation of 30 clusters of networks. Among the 30 clusters, clusters 1, 5, 6, and 12 offer data for functional enrichment analysis (Figure 4.35). In cluster 1, proteins are localised at the plasma membrane and are involved in the biological processes of cell surface receptor signalling, regulation of cell adhesion, apoptotic process, positive regulation of MAPK cascade, and negative regulation of cell population proliferation. In addition, the proteins in cluster 1 are linked to KEGG pathways that are specifically relevant to hematopoietic cell lineage and MAPK signalling pathways. The genes of major importance include TNF and IL1B, which play roles in nearly all biological processes and pathways. Furthermore, proteins found in clusters 6 and 12 are specifically located in plasma membrane region. These proteins have a role in the molecular function of transmembrane transporter activity, specifically in ABC transporters and the Ras signalling pathway.

Figure 4.36 reveals the presence of eleven clusters in the downregulated genes of K562-r cells transfected with hsa-miR-3131. Proteins in cluster 1 were located near the cellular membrane and played a role in regulating cell adhesion. Additionally, it was revealed that cluster 9 proteins are engaged in KEGG pathways related to cell adhesion molecules, as well as biological processes such as stem cell proliferation and Wnt signalling.

Finally, k562-r cells that were transfected with osa-mir1858a/b only produced a single cluster from the upregulated genes (Figure 4.37). Proteins in cluster 1 are situated at the outer surface of cells and have a role in controlling the growth of cell populations and the MAPK signalling pathway. Furthermore, the proteins also participate in the TNF signalling pathway and hematopoietic cell lineage with IL1B and IL1A. Table 4.27

– 4.33 summarised the functional enrichment analysis of microarray genes from hsa-miR-3131 and osa-mir1858a/b treated groups in both cells.

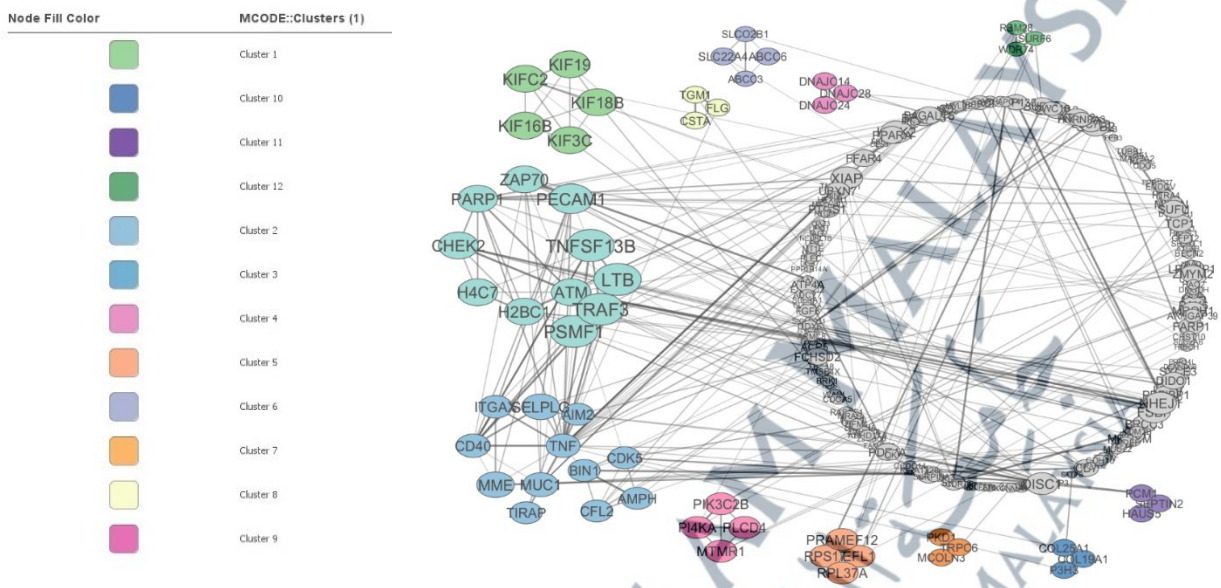

Figure 4.31: Protein–protein interaction (PPI) network clustering of upregulated genes of hsa-miR-3131 in K562-s showing 12 clusters. The network was generated and visualised in Cytoscape. Clusters were identified using the MCODE plugin, with node colours representing distinct functional modules and node size indicating connection degree.

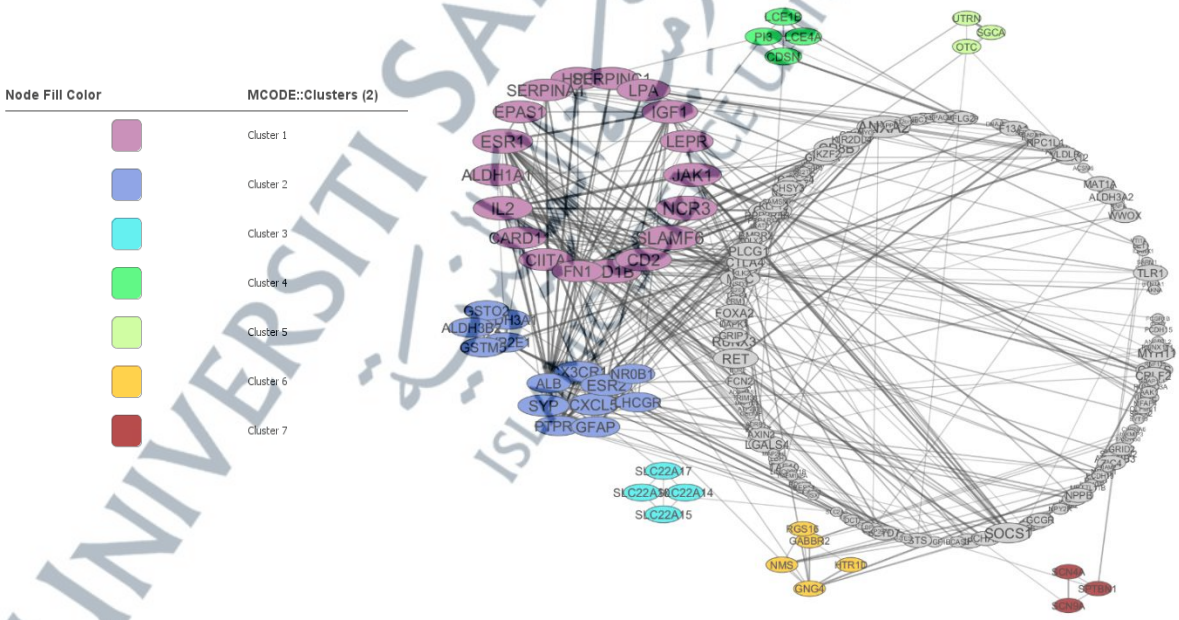

Figure 4.32: Protein–protein interaction (PPI) network clustering of downregulated genes of hsa-miR-3131 in K562-s showing seven clusters. The network was generated and visualised in Cytoscape. Clusters were identified using the MCODE plugin, with

node colours representing distinct functional modules and node size indicating connection degree.

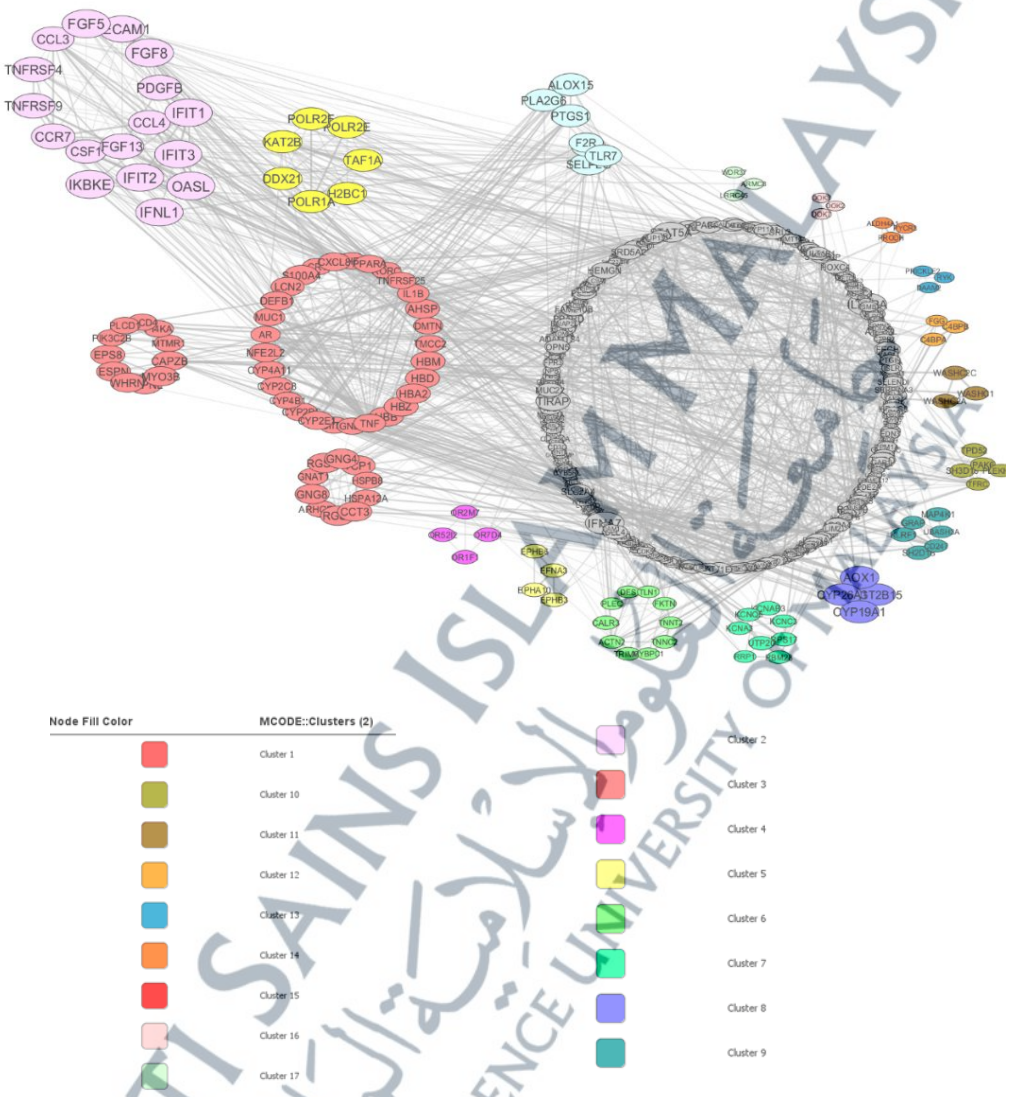

Figure 4.33**:** Protein–protein interaction (PPI) network clustering of upregulated genes of osa-miR1858a/b in K562-s showing 17 clusters. The network was generated and visualised in Cytoscape. Clusters were identified using the MCODE plugin, with node colours representing distinct functional modules and node size indicating connection degree.

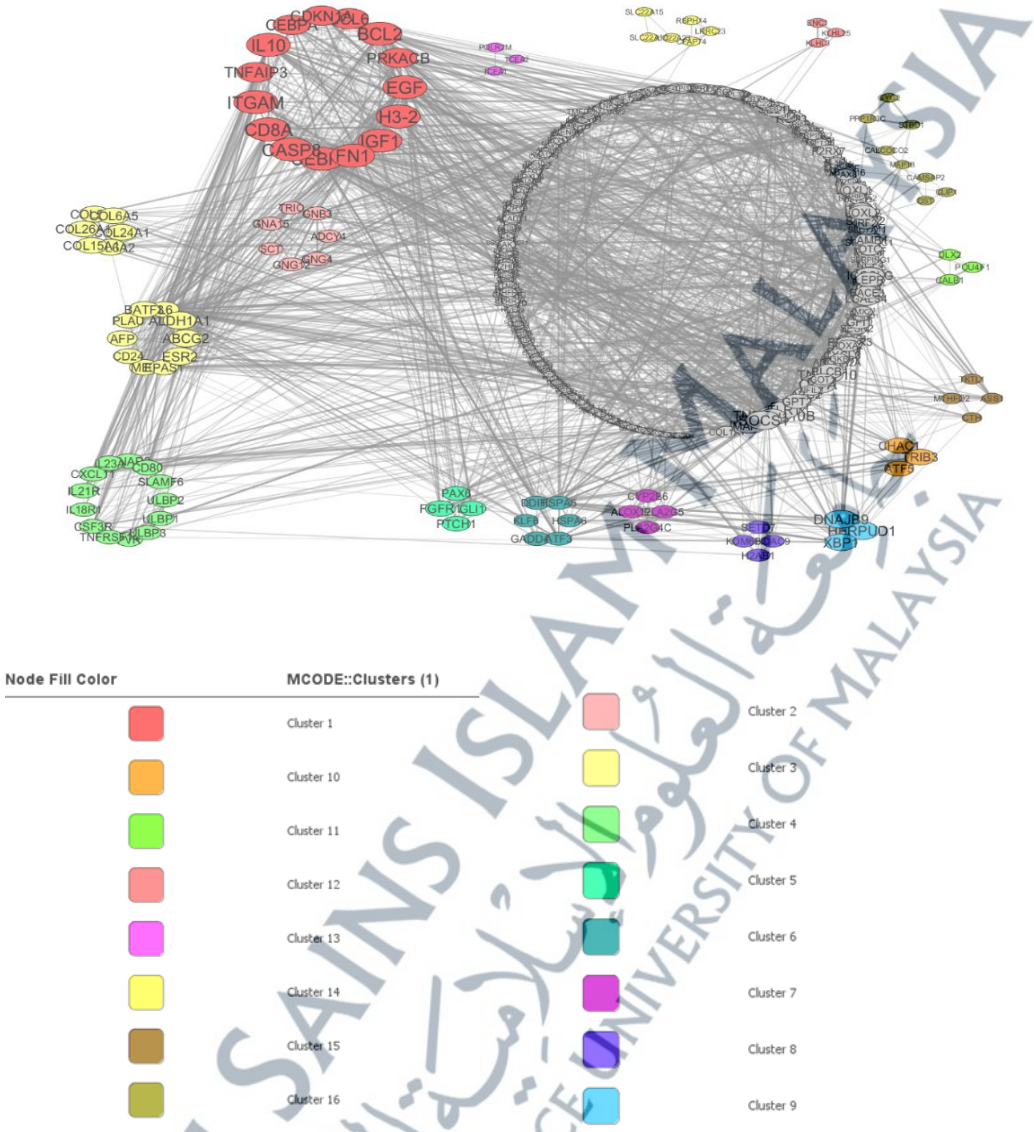

Figure 4.34: Protein–protein interaction (PPI) network clustering of downregulated genes of osa-miR1858a/b in K562-s showing 16 clusters. The network was generated and visualised in Cytoscape. Clusters were identified using the MCODE plugin, with node colours representing distinct functional modules and node size indicating connection degree.

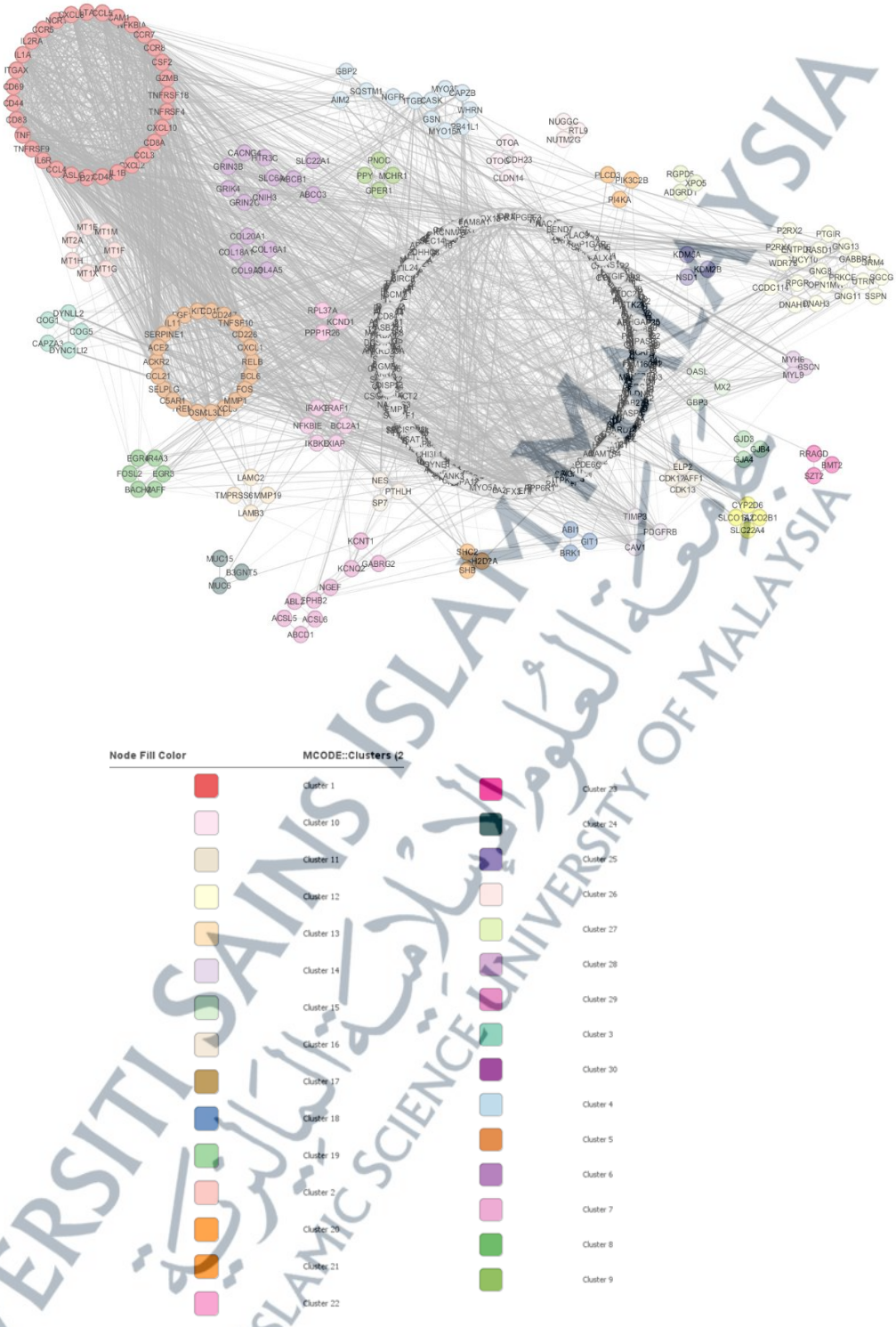

Figure 4.35: Protein–protein interaction (PPI) network clustering of upregulated genes of hsa-miR-3131 in K562-r showing 30 clusters. The network was generated and visualised in Cytoscape. Clusters were identified using the MCODE plugin, with node colours representing distinct functional modules and node size indicating connection degree.

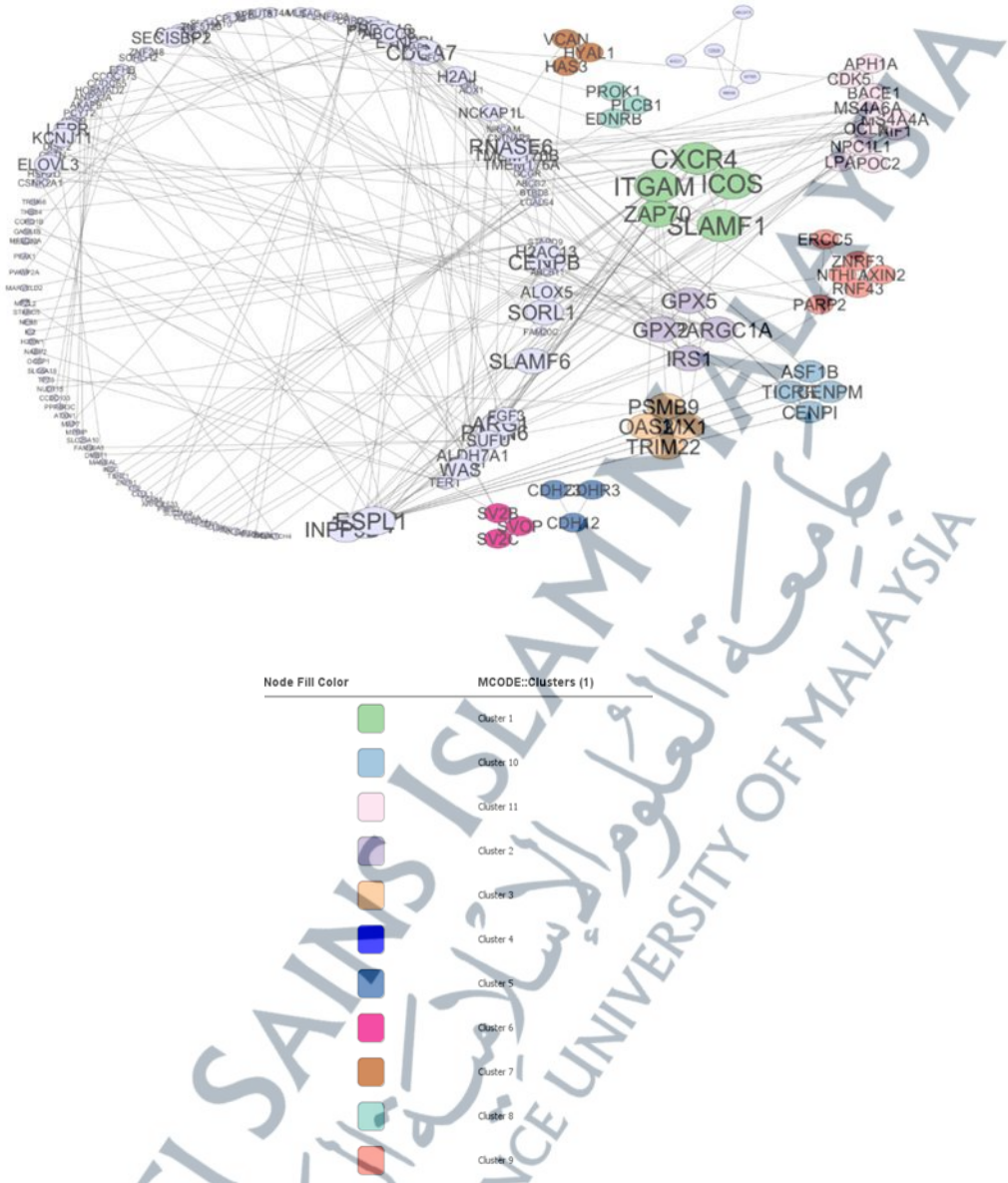

Figure 4.36: Protein–protein interaction (PPI) network clustering of downregulated genes of hsa-miR-3131 in K562-r showing 11 clusters. The network was generated and visualised in Cytoscape. Clusters were identified using the MCODE plugin, with node colours representing distinct functional modules and node size indicating connection degree.

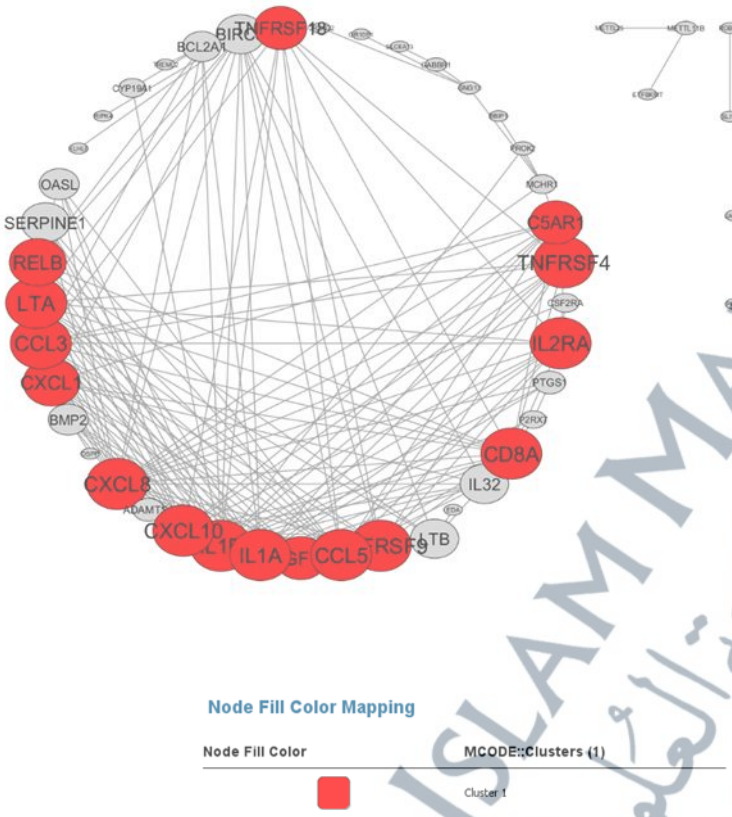

Figure 4.37: Protein–protein interaction (PPI) network clustering of upregulated genes of osa-mir1858a/b in K562-r showing one clusters. The network was generated and visualised in Cytoscape. Clusters were identified using the MCODE plugin, with node colours representing distinct functional modules and node size indicating connection degree.

Table 4.27: Functional enrichment analysis of microarray genes from hsa-miR-3131 and osa-mir1858a/b.

Cell	miRNA	Cluster	Category	Description	*Genes*	p-value
K562-s	Hsa-miR-3131 upregulated genes	2	Reactome pathways	DNA Double-Strand Break Repair	*H2BC1, ATM, PARP1, CHEK2*	1.10E-06
				G2/M Checkpoints		1.10E-06
		3	KEGG pathways	Hematopoietic cell lineage	*TNF, MME*	0.0014
		6	Molecular function	Active ion transmembrane transporter activity	*SLC22A4, ABCC6, ABCC3, SLCO2B1*	3.71E-08
			KEGG pathways	ABC transporters	*ABCC6, ABCC3,*	3.33E-05
	Hsa-miR-3131 downregulated genes	1	Biological process	Positive regulation of cell-cell adhesion	*IL2, IGF1, CARD11, JAK1*	1.90E-04
			Cellular component	Extracellular region	*IL2, HPX, ALDH1A1, LPA, LEPR, FN1, SERPINC1, SLAMF6, CD1B, CD2, IGF1, CARD11, SERPINA1*	5.07E-06
			KEGG pathways	PI3K-Akt signalling pathway	*IL2, FN1, IGF1, JAK1*	2.50E-04
				JAK-STAT signalling pathway	*IL2, LEPR, JAK1*	4.00E-04

Table 4.28: Functional enrichment analysis of microarray genes from hsa-miR-3131 and osa-mir1858a/b (continued).

Cell	miRNA	Cluster	Category	Description	*Genes*	p-value
K562-s	Osa-mir1858a/b upregulated genes	1	Compartme-nts	Nucleus	*KAT2B, POLR1A, H2BC1, TAF1A, DDX21, POLR2F, POLR2E*	5.03E-05
		2	KEGG pathways	Ras signalling pathway	*FGF5, FGF8, CSF1, PDGFB*	3.75E-05
				MAPK signalling pathway		9.38E-05
				PI3K-Akt signalling pathway		2.00E-04
		3	Cellular component	Cytoplasm	*GNAT1, HBA2, HBZ, PI4KA, IL1B, HSPB8, CCT3, DEFB1, AHSP, CYP4A11, TCP1, CYP2B6, GHRL, ARHGEF1, ESPNL, HBM, TMCC2, WHRN, CR1, PIK3C2B, S100A4, CYP2C8, CYP4B1, LCN2, AR, TNFRSF25, NFE2L2, RGS11, MYO3B, PLCD4, TNF, CAPZB, MTMR1, DMTN, PLCD1, GNLY, CYP2E1, RGS6, MUC1, CIITA, HSPA12A, HBB, EPS8, HBD, ESPN*	5.79E-06
				Vesicle	*HBA2, HBZ, PI4KA, IL1B, CCT3, DEFB1, TCP1, GHRL, CR1, PIK3C2B, S100A4, LCN2, GNG4, TNF, CAPZB, DMTN, PLCD1, GNLY, MUC1, HSPA12A, HBB, EPS8*	1.10E-04
			KEGG Pathways	Pathways in cancer	*GNG8, CXCL8, ARHGEF1, AR, NFE2L2, GNG4*	0.0019
		13	KEGG pathways & biological process	Wnt signalling pathway	*DAAM2, RYK, PRICKLE2*	4.96E-07

Table 4.29: Functional enrichment analysis of microarray genes from hsa-miR-3131 and osa-mir1858a/b (continued).

Cell	miRNA	Cluster	Category	Description	*Genes*	p-value
K562-s	Osa-mir1858a/b downregulated genes	1	Biological process	Regulation of cell population proliferation	*EGF, CEBPB, FN1, IGF1, BCL2, BCL6, CDKN1A, IL10, CEBPA, TNFAIP3*	3.94E-08
				Regulation of cell cycle	*EGF, IGF1, BCL2, BCL6, CDKN1A, IL10, CEBPA, TNFAIP3*	
				Regulation of apoptotic process	*CEBPB, CASP8, IGF1, BCL2, BCL6, IL10, TNFAIP3, ITGAM*	
				Hemopoiesis	*CEBPB, CASP8, BCL2, BCL6, CD8A, IL10, CEBPA*	2.37E-07
			KEGG pathways	Pathways in cancer	*EGF, FN1, CASP8, PRKACB, IGF1, BCL2, CDKN1A, CEBPA*	1.27E-09
				FoxO signalling pathway	*EGF, IGF1, BCL6, CDKN1A, IL10*	3.42E-08
				PI3K-Akt signalling pathway	*EGF, FN1, IGF1, BCL2, CDKN1A*	4.70E-06
				p53 signalling pathway	*CASP8, IGF1, BCL2, CDKN1A*	2.70E-07
				JAK-STAT signalling pathway	*EGF, BCL2, CDKN1A, IL10*	5.59E-06
		2	KEGG pathways	Pathways in cancer	*GNB3, ADCY4, GNG12, GNG4*	1.56E-05
				Ras signalling pathway	*GNB3, GNG12, GNG4*	5.17E-05
				PI3K-Akt signalling pathway		1.90E-04

Table 4.30: Functional enrichment analysis of microarray genes from hsa-miR-3131 and osa-mir1858a/b (continued).

Cell	miRNA	Cluster	Category	Description	*Genes*	p-value
K562-s	Osa-mir1858a/b downregulated genes	3	KEGG pathways	PI3K-Akt signalling pathway	*COL6A5, COL6A2, MET, IL6*	1.60E-04
				Pathways in cancer	*EPAS1, MET, ESR2, IL6*	6.70E-04
		4	Cellular component	External side of plasma membrane	*ULBP1, CD80, IL21R, TNFRSF14, ULBP3, ULBP2, SLAMF6, CSF3R*	2.92E-11
				Cell surface	*ULBP1, CD80, IL21R, TNFRSF14, ULBP3, ULBP2, SLAMF6, CSF3R, PVR*	5.18E-10
				Plasma membrane	*IL23A, ULBP1, CD80, IL21R, IFNAR2,*	2.40E-06
				Intrinsic component of membrane	*TNFRSF14, ULBP3, ULBP2, SLAMF6, CSF3R, IL18R1, PVR*	4.29E-06
			KEGG pathways	JAK-STAT signalling pathway	*IL23A, IL21R, IFNAR2, CSF3R*	2.97E-06
		6	KEGG pathways	MAPK signalling pathway	*GADD45B, HSPA6, DDIT3*	6.04E-05
				Apoptosis	*GADD45B, DDIT3*	6.70E-04
K562-r	Hsa-miR-3131 upregulated genes	1	Biological process	Cell surface receptor signalling pathway	*NFKBIA, CCR7, IL1A, IL1B, CCR5, CSF2, CXCL10, CXCL8, CD276, CCR8, TNFRSF18, FASLG, IL6R, TNFRSF4, IL2RA, CD8A, CD44, TNF, CXCL2, ITGAX, CCL5, CCL3, CCL4*	8.55E-17
				Regulation of cell adhesion	*CCR7, IL1A, IL1B, CXCL8, CD276, TNFRSF18, IL6R, CD83, IL2RA, CD44, TNF, CCL5*	1.19E-09
				Apoptotic process	*GZMB, NFKBIA, IL1A, IL1B, TNFRSF18, FASLG, IL6R, IL2RA, TNF, LTA, TNFRSF9*	2.97E-07

Table 4.31: Functional enrichment analysis of microarray genes from hsa-miR-3131 and osa-mir1858a/b (continued).

Cell	miRNA	Cluster	Category	Description	*Genes*	p-value
K562-r	Hsa-miR-3131 upregulated genes	1	Biological process	Positive regulation of MAPK cascade	*CCR7, IL1A, IL1B, ICAM1, IL6R, CD44, TNF, CCL5, CCL3, CCL4*	2.31E-09
				Negative regulation of cell population proliferation	*IL1A, IL1B, CXCL8, IL2RA, TNF, LTA, TNFRSF9*	1.00E-04
			Cellular component	Plasma membrane	*GZMB, NFKBIA, CD69, CCR7, IL1A, ICAM1, NCR1, CCR5, CSF2, CXCL10, CD276, CCR8, TNFRSF18, FASLG, IL6R, CD83, TNFRSF4, IL2RA, CD8A, CD44, TNF, LTA, ITGAX, TNFRSF9, CD48*	1.98E-09
			KEGG pathways	Hematopoietic cell lineage	*IL1A, IL1B, CSF2, IL6R, IL2RA, CD8A, CD44, TNF*	1.99E-12
				MAPK signalling pathway	*IL1A, IL1B, FASLG, TNF*	0.0011
		5	Biological process	Regulation of MAPK cascade	*OSM, CCL21, IL11, KIT, C5AR1, ACE2, CCL3L1*	5.81E-06
				Myeloid cell differentiation	*RELB, IL11, KIT, FOS, BCL6*	9.73E-06
			KEGG pathways	Hematopoietic cell lineage	*IL11, KIT, CD1B*	1.50E-04
				TNF signalling pathway	*CXCL3, FOS, CXCL1*	2.70E-04
		6	Cellular component	Plasma membrane region	*GRIN3B, SLC6A4, CACNG4, CNIH3, ABCC3, GRIN2C, SLC22A1, GRIK4, ABCB1*	5.53E-08

Table 4.32: Functional enrichment analysis of microarray genes from hsa-miR-3131 and osa-mir1858a/b (continued).

Cell	miRNA	Cluster	Category	Description	*Genes*	p-value
K562-r	Hsa-miR-3131 upregulated genes	6	Molecular function	Transmembrane transporter activity	*GRIN3B, SLC6A4, CACNG4, ABCC3, GRIN2C, HTR3C, SLC22A1, GRIK4, ABCB1*	2.37E-08
			KEGG pathways	ABC transporters	*ABCC3, ABCB1*	5.70E-04
		12	Cellular component	Plasma membrane	*SGCG, P2RX1, RASD1, SSPN, GNG13, GNG11, PTGIR, GNG8, ENTPD3, PRKCE, P2RX2, UTRN, ADCY10, GABBR1, GRM4, OPN1MW*	6.89E-06
			KEGG pathways	Ras signalling pathway	*GNG13, GNG11, GNG8*	0.0017
	Hsa-miR-3131 downregulated genes	1	Cellular component	Side of membrane	*ZAP70, CXCR4, SLAMF1, ITGAM*	4.58E-06
			Biological process	Regulation of cell adhesion	*ZAP70, ICOS, CXCR4, SLAMF1*	1.23E-05
				Cell adhesion	*ZAP70, ICOS, SLAMF1, ITGAM*	2.79E-05
		9	KEGG pathways	Cell adhesion molecules	*ICOS, ITGAM*	4.90E-04
			Biological process	Stem cell proliferation	*AXIN2, ZNRF3, RNF43*	1.33E-06
			KEGG pathways	Wnt signalling pathway		9.75E-06
	osa-mir1858a/b upregulated genes	1	Cellular component	Cell surface	*IL1A, CXCL10, TNFRSF18, TNFRSF4, IL2RA, CD8A, TNFRSF9*	3.24E-06
			Biological process	Positive regulation of cell population proliferation	*IL1A, IL1B, CXCL10, C5AR1, TNFRSF4, IL2RA, LTA, CCL5*	2.63E-07

Table 4.33: Functional enrichment analysis of microarray genes from hsa-miR-3131 and osa-mir1858a/b (continued).

Cell	miRNA	Cluster	Category	Description	*Genes*	p-value
K562-r	osa-mir1858a/b upregulated genes	1	Biological process	Negative regulation of cell population proliferation	*IL1A, IL1B, CXCL8, IL2RA, CXCL1, LTA, TNFRSF9*	7.22E-07
				Positive regulation of MAPK cascade	*IL1A, IL1B, C5AR1, CCL5, CCL3*	3.11E-05
			KEGG pathways	TNF signalling pathway	*IL1B, CXCL10, CXCL1, LTA, CCL5*	2.68E-08
				Hematopoietic cell lineage	*IL1A, IL1B, IL2RA, CD8A*	8.44E-07